

DESY 97-125  
HUB-EP-97/38  
June 1997

## Scaling of Non-Perturbatively $O(a)$ Improved Wilson Fermions: Hadron Spectrum, Quark Masses and Decay Constants

M. Göckeler<sup>1</sup>, R. Horsley<sup>2</sup>, H. Perlt<sup>3</sup>, P. Rakow<sup>4</sup>,  
G. Schierholz<sup>4,5</sup>, A. Schiller<sup>3</sup> and P. Stephenson<sup>4</sup>

<sup>1</sup> Institut für Theoretische Physik, Universität Regensburg,  
D-93040 Regensburg, Germany

<sup>2</sup> Institut für Physik, Humboldt-Universität,  
D-10115 Berlin, Germany

<sup>3</sup> Institut für Theoretische Physik, Universität Leipzig,  
D-04109 Leipzig, Germany

<sup>4</sup> Deutsches Elektronen-Synchrotron DESY,  
Institut für Hochenergiephysik und HLRZ,  
D-15735 Zeuthen, Germany

<sup>5</sup> Deutsches Elektronen-Synchrotron DESY,  
D-22603 Hamburg, Germany

### Abstract

We compute the hadron mass spectrum, the quark masses and the meson decay constants in quenched lattice QCD with non-perturbatively  $O(a)$  improved Wilson fermions. The calculations are done for two values of the coupling constant,  $\beta = 6.0$  and  $6.2$ , and the results are compared with the predictions of ordinary Wilson fermions. We find that the improved action reduces lattice artifacts as expected.

# 1 Introduction

The calculation of hadron masses in lattice gauge theory has a long history. Over the years there has been a steady improvement in computing power and methods allowing simulations on larger volumes and smaller quark masses with higher statistics. However, the progress to smaller lattice spacing  $a$  has been slower because of the high computer cost which increases by at least a factor of  $(1/a)^5$ . Since it is so expensive to reduce cut-off effects by reducing  $a$ , we should consider reducing them by improving the action.

A systematic improvement program reducing the cut-off errors order by order in  $a$  has been proposed by Symanzik [1] and developed for on-shell quantities in ref. [2]. The standard gluonic action has discretization errors of  $O(a^2)$ , but those for Wilson fermions are of  $O(a)$ . Therefore it is the fermionic action which is most in need of improvement.

Sheikholeslami and Wohlert [3] proposed the action (we assume  $r = 1$  throughout the paper)

$$S_F = S_F^{(0)} - \frac{i}{2} \kappa g c_{SW}(g) a^4 \sum_x \bar{\psi}(x) \sigma_{\mu\nu} F_{\mu\nu}(x) \psi(x), \quad (1)$$

where  $S_F^{(0)}$  is the original Wilson action and

$$F_{\mu\nu}(x) = \frac{1}{8iga^2} \sum_{\mu, \nu = \pm} (U(x)_{\mu\nu} - U(x)_{\mu\nu}^\dagger). \quad (2)$$

In eq. (2) the sum extends over the four plaquettes in the  $\mu\nu$ -plane which have  $x$  as one corner, and the plaquette operators  $U(x)_{\mu\nu}$  are the products of the four link matrices comprising the plaquettes taken in a clockwise sense. If  $c_{SW}$  is appropriately chosen, this action removes all  $O(a)$  errors from on-shell quantities such as the hadron masses. A non-perturbative evaluation of this function leads to [4]

$$c_{SW}(g) = \frac{1 - 0.656 g^2 - 0.152 g^4 - 0.054 g^6}{1 - 0.922 g^2}, \quad g^2 \leq 1. \quad (3)$$

When we talk about improved fermions in the following, we always understand that  $c_{SW}$  has been chosen according to eq. (3).

In this paper we shall present results for the light hadron mass spectrum, the light and strange quark masses and the light meson decay constants using the improved action. The calculation is done for two values of the coupling,  $\beta = 6.0$  and  $6.2$ , which allows us to test for scaling.

The mass calculations extend our earlier work [5] where we have examined the  $c_{SW}$  dependence at  $\beta = 6.0$ . To exhibit the effect of improvement, we have also done calculations with Wilson fermions on the same lattices. Most of our Wilson data come from our structure function calculations [6, 7], and we combine this with masses from the literature at other  $\beta$  values to see the dependence on  $a$  clearly.

From the meson correlation functions we also extract meson decay constants and quark masses. However, simply improving the action is not sufficient to remove all  $O(a)$  errors from these quantities. Here we also have to improve the operators which is done by adding higher dimensional terms with the same quantum numbers in an appropriate fashion.

This paper is organized as follows. In sec. 2 we briefly describe our numerical method. The hadron masses are given in sec. 3, concentrating in particular on the extrapolation to the chiral limit and the scaling behavior of improved and Wilson action results. In sec. 4 we compute the light and strange quark masses using two different methods, from the axial vector current Ward identity and from the lattice bare quark masses. The meson decay constants are discussed in sec. 5. Finally, in sec. 6 we give our conclusions.

## 2 Computational Details

Our calculations have mainly been done at  $\beta = 6.0$  and  $6.2$  on  $16^3 32$ ,  $24^3 32$  and  $24^3 48$  lattices. We use Quadrics (formerly called *APE*) parallel computers. For the improved case the parameter  $c_{SW}$  is given from eq. (3) as  $c_{SW} = 1.769$  at  $\beta = 6.0$  and  $c_{SW} = 1.614$  at  $\beta = 6.2$ . The simulations are done for at least five different  $\kappa$  values in each case. This helps with the extrapolation to the chiral limit.

For the gauge field update we use a combination of 16 overrelaxation sweeps followed by a three-hit Metropolis update. This procedure is repeated 50 times to generate a new configuration.

The improvement term in eq. (1) appears in the site-diagonal part of the action. The major overhead in our case is multiplication by this term during inversion of the fermion mass matrix. In our basis of hermitean gamma matrices we can rewrite this term as [8]

$$\begin{aligned} 1 - \frac{i}{2} \kappa g c_{SW} \sigma \cdot F &= \begin{pmatrix} A & B \\ B & A \end{pmatrix} \\ &= \frac{1}{2} \begin{pmatrix} 1 & -1 \\ 1 & 1 \end{pmatrix} \begin{pmatrix} A+B & 0 \\ 0 & A-B \end{pmatrix} \begin{pmatrix} 1 & 1 \\ -1 & 1 \end{pmatrix}, \end{aligned} \quad (4)$$

where  $A, B$  are  $6 \times 6$  matrices (two-spinors with color), so that instead of a  $12 \times 12$  multiplication we have two  $6 \times 6$  multiplications and two inexpensive coordinate transformations. This reduces the overhead for the improvement in the inverter from 45% to 30%. Also, the inverse of the matrix in eq. (4) is required on half the lattice due to the even-odd preconditioning. We now have to invert two  $6 \times 6$  instead of a  $12 \times 12$  matrix. However, this is only required once for each propagator inversion.

For the matrix inversion we mainly used the minimal residue algorithm, except for the lightest quark mass on the larger lattices where we used the BiCGstab algorithm [9, 10]. As convergence criterion we chose

$$|r| \leq 10^{-6} \quad (5)$$

for the residue, which is the best that can be achieved for our single precision machine.

For the mass calculations we used Jacobi smearing for source and sink. For a detailed description of our application of this procedure see ref. [11]. We have two parameters we can use to set the size of our source, the number of smearing steps,  $N_s$ , and the smearing hopping parameter,  $\kappa_s$ . We chose  $N_s = 50$  for  $\beta = 6.0$  and 100 for  $\beta = 6.2$  and  $\kappa_s = 0.21$  at both  $\beta$  values. This gives roughly the same r.m.s. radius in physical units in both cases, namely 0.4 fm. To define the matrix elements for the decay constants and quark masses, we have also computed correlation functions with smeared source and local sink. This does not require any additional matrix inversions.

At  $\beta = 6.0$  and  $c_{SW} = 0$  we had generated  $O(5000)$  configurations for our structure function project on which we have computed the hadron masses. To these we added  $O(150)$  new configurations on which we computed the meson decay constants and the chiral Ward identity. For  $c_{SW} = 1.769$  we have analyzed  $O(1000)$  configurations. For the heavier quark masses,  $\kappa = 0.1487$  and  $\kappa = 0.1300, 0.1310, 0.1320$ , respectively, the number of configurations was  $O(200)$ . On the  $24^3$  lattice we have generated  $O(100)$  and  $O(200)$  configurations at  $c_{SW} = 0$  and 1.769, respectively. At  $\beta = 6.2$  we only ran on  $24^3$  lattices. Here we have analyzed  $O(100)$  configurations for  $c_{SW} = 0$  and  $O(300)$  configurations for  $c_{SW} = 1.614$ . We employed both relativistic and non-relativistic wave functions [6, 7], except for the high statistics runs where we only looked at the non-relativistic wave function in order to save computer time.

Besides our calculations at  $\beta = 6.0$  and 6.2 we also made exploratory studies at  $\beta = 5.7$  to see what effect varying  $c_{SW}$  has on coarser lattices. If one decreases  $\beta$ , increases  $c_{SW}$  or increases  $\kappa$ , one starts to get problems with exceptional configurations. This showed up in non-convergence of our fermion matrix inversions. It was, however, only a real problem at  $\beta = 5.7$ ,  $c_{SW} = 2.25$  and [5]  $\beta = 6.0$ ,  $c_{SW} = 3.0$ .

### 3 Hadron Masses

We consider hadrons where all the quarks have degenerate masses. We looked at  $\pi$ ,  $\rho$ , nucleon ( $N$ ),  $a_0$ ,  $a_1$  and  $b_1$  masses, and we have used this nomenclature for all quark masses, not just in the chiral limit.

In our mass calculations we have made single exponential fits to meson and baryon correlators over appropriate fit ranges. The errors are determined using the bootstrap method with 50 data samples. We present our hadron mass results in tables 1, 2 and 3. Table 2 updates the results presented in ref. [5]. For the meson masses we found very little difference between using relativistic and non-relativistic wave functions, and we settled for relativistic wave functions (except for the high statistics runs). For the nucleon we have chosen non-relativistic wave functions [6] which performed slightly better because the effective mass plateaus extended to larger times. At  $\beta = 6.0$  we repeated the lightest quark mass on  $16^3 32$

on the  $24^3 32$  lattice, for both improved and Wilson fermions. The values agree within less than 3%. This indicates that all our results on the  $16^3 32$  lattice do not suffer from significant finite size effects.

### *Chiral Behavior*

To obtain the critical value of  $\kappa$ ,  $\kappa_c$ , and the hadron masses in the chiral limit, we extrapolate our data to zero  $\pi$  mass. We first tried

$$m_\pi^2 = b \left( \frac{1}{\kappa} - \frac{1}{\kappa_c} \right). \quad (6)$$

Using this relation gives a rather poor fit of the data, and we saw that there was a slight curvature in a plot of  $m_\pi^2$  against  $1/\kappa$ . Quenched chiral perturbation theory predicts [12]

$$m_\pi^2 = b' \left( \frac{1}{\kappa} - \frac{1}{\kappa_c} \right)^{\frac{1}{1+\delta}}, \quad (7)$$

where  $\delta$  is small and positive. We made fits using this formula but found that  $\delta$  was always negative. As in our previous work [5] we conclude that our  $\kappa$  values are too far from  $\kappa_c$  for the formula to be applicable. This is in agreement with observations made by other authors [13]. As an alternative parameterization of the curvature we used the phenomenological fit

$$\frac{1}{\kappa} = \frac{1}{\kappa_c} + b_2 m_\pi^2 + b_3 m_\pi^3. \quad (8)$$

In table 4 we give the values of  $\kappa_c$  for the different fits. The linear fits give  $\chi^2/\text{dof}$  values of up to 40. The other two fits both give acceptable values of  $\chi^2$ , but eq. (8) usually gives a lower  $\chi^2$  than eq. (7). In the following we shall take  $\kappa_c$  from the phenomenological fits.

In fig. 1 we plot  $\kappa_c$  for improved Wilson fermions. We compare our results with the results of ref. [4]. The agreement is excellent. In one-loop perturbation theory  $\kappa_c$  is given by [5]

$$\kappa_c = \frac{1}{8} [1 + g^2 (0.108571 - 0.028989 c_{SW} - 0.012064 c_{SW}^2)]. \quad (9)$$

The tadpole improved value of  $\kappa_c$  that follows from this result is

$$\kappa_c = \frac{1}{8} [1 + g^{*2} (0.025238 - 0.028989 c_{SW} u_0^3 - 0.012064 (c_{SW} u_0^3)^2)] u_0^{-1}, \quad (10)$$

where  $c_{SW}$  is given by eq. (3),

$$u_0 = \left\langle \frac{1}{3} \text{Tr} U_\square \right\rangle^{\frac{1}{4}} \quad (11)$$

and  $g^{*2}$  is the boosted coupling constant defined by

$$g^{*2} = g^2 / u_0^4. \quad (12)$$

In fig. 1 we compare the tadpole improved perturbative formula (10) with the data where for the larger couplings we have taken  $u_0$  from [14, 15]. The curve and the data points agree within less than 1%. In eq. (10) one has the choice of using the lowest order tadpole improved value of  $c_{SW}$ , namely  $u_0^{-3}$  [4], or the value from eq. (3) which is the value actually used in the simulations. Both procedures remove all the tadpole diagrams and differ only by small  $O(g^4)$  terms, so they are both reasonable. We prefer the second choice.

We fit the other hadron masses by the formula

$$m_H^2 = b_0 + b_2 m_\pi^2 + b_3 m_\pi^3, \quad H = \rho, N, \dots \quad (13)$$

The result of the fit is shown in fig. 2 for both improved and Wilson fermion data. The Wilson fermion data are the world data compiled in tables 5, 6 and 7.

We find this to be a more appropriate fit formula than the ansatz [26]

$$m_H = b'_0 + b'_2 m_\pi^2 + b'_3 m_\pi^3, \quad (14)$$

because for the nucleon the plot of  $m_N^2$  against  $m_\pi^2$  (or  $1/\kappa$ ) is less curved than  $m_N$  against  $m_\pi^2$ . (Note that the two formulae differ only by terms of  $O(m_\pi^4)$ ). To decide which fit formula is best and to do a reliable extrapolation to the chiral limit, it is important to have many  $\kappa$  values. For the  $a_0$ ,  $a_1$  and  $b_1$  masses only a two-parameter fit with  $b_3$  set to zero was reasonable. The mass values in the chiral limit for our data are also given in tables 1, 2 and 3.

We see that the effect of improvement is largest for the  $\rho$  mass. In the chiral limit the difference between improved and Wilson results is 25% at  $\beta = 6.0$  and still 12% at  $\beta = 6.2$ . It is quite common to define the physical scale from the  $\rho$  mass. The relatively large change of this quantity from the Wilson to the improved case suggests that it contains large  $O(a)$  corrections, and that this procedure is misleading. A better procedure is to use the string tension or  $r_0$  [27], the force parameter, as the scale. For the nucleon mass the difference between the two actions is smaller.

## *APE Plots*

In figs. 3 and 4 we show the dimensionless ratio  $m_N/m_\rho$  as a function of  $(m_\pi/m_\rho)^2$ , a so-called *APE* plot, for  $\beta = 6.0$  and 6.2, both for improved and Wilson fermions (the latter using the world data given in tables 5 and 6). The solid lines are the results of the ratio of the fits in fig. 2. At  $\beta = 6.0$  we find that the mass ratio data are rather different for the two actions. The improved results lie consistently lower than the Wilson results. At  $\beta = 6.2$  we find the same pattern in the data.

At  $\beta = 6.0$  we can say something about the chiral limit. Our fits give  $m_N/m_\rho = 1.20(6)$  for improved fermions and  $m_N/m_\rho = 1.33(2)$  for Wilson fermions. The improved results come closer to the physical value than the Wilson results. At  $\beta = 6.2$  we are lacking data at

small quark masses and on larger volumes. In the chiral limit our fits give  $m_N/m_\rho = 1.32(11)$  for improved fermions and  $m_N/m_\rho = 1.39(12)$  for Wilson fermions, so that we cannot say anything conclusive about the behavior of the two actions in the chiral limit in this case.

### *Scaling Behavior*

Let us now look at and compare the scaling behavior of the two actions. We shall limit our discussion to the  $\rho$  mass because the errors of the nucleon are too large to make precise statements. In order to exhibit the cut-off effects most clearly, it has been suggested [28] that  $m_\rho$  should be plotted in units of the square-root of the string tension  $K$  which has cut-off errors of  $O(a^2)$  only. In table 8 we have compiled the world string tension data. When there are several calculations, we performed the weighted average.

In fig. 5 we plot the ratio  $m_\rho/\sqrt{K}$  as a function of  $a\sqrt{K}$ . This is done for fixed physical  $\pi$  masses with  $m_\pi^2 = 0, 2K$  and  $4K$ . Comparing hadron masses at larger quark masses has the advantage that this does not require large extrapolations of the lattice data but rather involves small interpolations only. The Wilson fermion data shown are a fit to the world data compiled in tables 5, 6 and 7. As expected, the Wilson masses show practically a linear behavior in the lattice spacing  $a$ . We have done a simultaneous linear plus quadratic fit to the Wilson data and a quadratic fit to the improved data. The fit is constrained to agree in the continuum limit. The result of the fit is shown by the solid lines in fig. 5. In the continuum limit we obtain  $m_\rho/\sqrt{K} = 1.80(10)$ . We compare this result with the experimental  $\rho$  mass. For the string tension we take the value

$$\sqrt{K} = 427 \text{ MeV} \tag{15}$$

which has been obtained from a potential fit to the charmonium mass spectrum [36]. Using this value the physical  $m_\rho/\sqrt{K}$  is 1.80 which agrees with the lattice number.

As mentioned previously, an alternative scale from the potential is  $r_0$ . We have also compiled lattice results for  $r_0$  in table 8. We see that it scales very well with  $\sqrt{K}$ , as the product  $r_0\sqrt{K}$  is approximately constant at about 1.19, while the lattice spacing  $a$  changes by a factor of more than five. However, the physical value of  $r_0\sqrt{K}$  is 1.06, taking  $r_0^{-1}$  as 402 MeV which follows from the same potential that gives  $\sqrt{K} = 427 \text{ MeV}$  [36]. It does not seem that this discrepancy will vanish as  $a \rightarrow 0$ . It is telling us that the lattice potential has a slightly different shape to the continuum potential. This may be an effect of quenching [37].

Although at  $\beta = 5.7$  we do not know the correct value of  $c_{SW}$ , using our larger value  $c_{SW} = 2.25$  we find  $m_\rho/\sqrt{K} = 1.94$  in the chiral limit. Comparing this number with fig. 5, it indicates that  $O(a^2)$  effects are moderate even at this coupling.

## Mass Splitting

The vector-pseudoscalar mass splitting

$$\Delta_{V-PS} = m_V^2 - m_{PS}^2 \quad (16)$$

is experimentally rather constant for all quark flavors. One finds

$$\begin{aligned} m_\rho^2 - m_\pi^2 &= 0.57 \text{ GeV}^2, \\ m_{K^*}^2 - m_K^2 &= 0.55 \text{ GeV}^2, \\ m_{D^*}^2 - m_D^2 &= 0.55 \text{ GeV}^2. \end{aligned} \quad (17)$$

Quenched lattice calculations with Wilson fermions are unable to reproduce these numbers. Wilson fermions give a splitting which is much too small. In fig. 6 we compare the experimental values of  $m_\rho^2 - m_\pi^2$  and  $m_{K^*}^2 - m_K^2$  with the lattice data and the mass fits. As before, we have taken the string tension eq. (15) as the scale. In fig. 6 we also show the results for improved fermions and the corresponding mass fits as well. There is a noticeable change when going to the improved case. We find good agreement with experiment for the absolute values.

In the heavy quark effective theory [38]

$$\Delta_{V-PS} \propto \langle \bar{\Psi} \sigma_{\mu\nu} F_{\mu\nu} \Psi \rangle, \quad (18)$$

where  $\Psi$  is the heavy quark field. So it is natural that turning on the Sheikholeslami-Wohlert term would increase the mass splitting, and this is what we see.

## Wilson $\kappa_c$

Let us now come back to the critical value of  $\kappa$  for Wilson fermions. In table 9 we have given the values of  $\kappa_c$  from a fit of the world data in tables 5, 6 and 7 using the phenomenological ansatz (8). In fig. 7 we plot these results as a function of  $a\sqrt{K}$  (the string tension being taken from table 8). We see that  $\kappa_c$  is a linear function of  $a$  over the whole range of the data which extends from  $\beta = 5.7$  to 6.4. Comparing this with the improved  $\kappa_c$ , which is approximately constant, we conclude that the Wilson  $\kappa_c$  has large  $O(a)$  effects. We also compare the Wilson data with the predictions of tadpole improved perturbation theory as given by eq. (10) with  $c_{SW} = 0$ . Here we have taken the one-loop perturbative formula for  $a$  beyond  $\beta = 6.8$  where there are no numerical values for the string tension available any more. Not even at the smallest value of  $a$  can perturbation theory describe the Wilson data. For improved fermions, on the other hand, the agreement with tadpole improved perturbation theory is quite good, as we have already noticed.



## 4 Quark Masses

We shall now turn to the calculation of the quark masses. When chiral symmetry is dynamically broken, care has to be taken in defining renormalized masses. In the continuum the renormalized quark mass at scale  $p^2 = \mu^2$  can be written [39]

$$\frac{1}{4}\text{Tr}[S_F^{-1}(m) - S_F^{-1}(0)] = m(\mu), \quad (19)$$

where  $S_F$  is the renormalized quark propagator which is to be evaluated in a given gauge. This definition refers to the momentum subtraction scheme. It is usual to give the quark masses in the  $\overline{MS}$  scheme. To convert from one scheme to the other, one has to go to high enough scales so that one can use perturbation theory. If the quark mass is defined in this way, then the renormalized mass is proportional to the bare mass.

On the lattice the standard assignment of the bare mass is

$$am(a) = \frac{1}{2} \left( \frac{1}{\kappa} - \frac{1}{\kappa_c} \right), \quad (20)$$

giving the renormalized mass as

$$m^{\overline{MS}}(\mu) = Z_m^{\overline{MS}}(a\mu, am) m(a), \quad (21)$$

where  $Z_m^{\overline{MS}}(a\mu, am)$  is the mass renormalization constant. We call this method of determining the renormalized mass the standard method.

An alternative way of defining a bare mass is by means of the *PCAC* relation between the divergence of the axial vector current  $A_\mu = \bar{\psi}\gamma_\mu\gamma_5\psi$  and the pseudoscalar density  $P = \bar{\psi}\gamma_5\psi$ ,

$$\tilde{m}(a) = \frac{\partial_4 \langle A_4(x) \mathcal{O} \rangle}{2 \langle P(x) \mathcal{O} \rangle}, \quad (22)$$

where  $\mathcal{O}$  is a suitable operator having zero three-momentum and no physical overlap with  $A_4(x)$  and  $P(x)$  to avoid contact terms. (See later on for a precise definition.) All operators are bare operators. To avoid anomaly terms in eq. (22), flavor non-singlet operators are taken. We call this method the Ward identity method. The renormalized mass is then given by

$$m^{\overline{MS}}(\mu) = \frac{Z_A(am)}{Z_P^{\overline{MS}}(a\mu, am)} \tilde{m}(a), \quad (23)$$

where  $Z_A(am)$  and  $Z_P^{\overline{MS}}(a\mu, am)$  are the renormalization constants of the axial vector current and the pseudoscalar density, respectively.

The quark mass inherits its scale dependence from the renormalization constants  $Z_m$  and  $Z_P$  which involve logarithms of  $\mu$ . In the following we will compute  $Z_m$  and  $Z_P$  perturbatively

to one-loop order for lack of a better, non-perturbative determination. To keep the logarithms under control it is best to take  $a\mu = 1$  and do the transformation to any other scale by the renormalization group formula

$$m^{\overline{MS}}(\mu') = \left( \frac{\alpha_s^{\overline{MS}}(\mu')}{\alpha_s^{\overline{MS}}(\mu)} \right)^{\frac{8}{22}} m^{\overline{MS}}(\mu). \quad (24)$$

In the continuum limit both procedures should give identical results for  $m^{\overline{MS}}(\mu)$ . Note, however, that the two bare masses  $m$  and  $\tilde{m}$  can be different, though they both vanish in the chiral limit. On the lattice the two procedures may give different results for  $m^{\overline{MS}}(\mu)$  due to non-universal discretization errors.

The lattice calculation of the quark masses now proceeds in two steps. In the first step one has to find the  $\kappa$  values corresponding to the real world by adjusting (e.g.) the pseudoscalar meson masses to their experimental numbers. In case of the Ward identity method one furthermore has to compute  $\tilde{m}$ . In the second step the bare quark masses have to be converted to renormalized masses. We shall compute the masses of the  $u$  and  $d$  quarks, which we assume to be equal, and the mass of the strange ( $s$ ) quark.

### *Improved Fermions*

Let us consider the case of improved fermions first. Later on we shall compare our results with the predictions of Wilson fermions to see the effect of improvement.

We will discuss the Ward identity method first. For the operator  $\mathcal{O}$  we take the pseudoscalar density

$$P(0) = \sum_{\vec{x}} P(x_4 = 0, \vec{x}) \quad (25)$$

and smear it as we did in the hadron mass calculations. As the  $P(0)$  part is common to all two-point functions, we could have used any operator projecting onto the pseudoscalar state. Similarly, we write

$$A_4(t) = \sum_{\vec{x}} A_4(x_4 = t, \vec{x}). \quad (26)$$

For improved fermions the axial vector current in eq. (22) is to be replaced by

$$A_4 \rightarrow A_4 + c_A a \partial_4 P(x), \quad (27)$$

where  $c_A$  is a function of the coupling only. The time derivative  $\partial_4$  is taken to be the average of the forward and backward derivative. The coefficient  $c_A$  has been computed in [4] giving  $c_A = -0.083$  at  $\beta = 6.0$  and  $c_A = -0.037$  at  $\beta = 6.2$ . The resulting bare mass

$$\tilde{m}(a) = \frac{\partial_4 \langle A_4(t) P(0) \rangle + c_A a \partial_4^2 \langle P(t) P(0) \rangle}{2 \langle P(t) P(0) \rangle} \quad (28)$$

has been plotted in fig. 8 for  $\beta = 6.0$  and our smallest quark mass on the  $16^3 32$  lattice. In fig. 9 we show the same quantity for  $\beta = 6.2$  and our smallest quark mass on the  $24^3 48$  lattice. (Also shown in these figures are the results for Wilson fermions which we will discuss later on.) Equation (28) should be independent of  $t$ , except where the operators physically overlap with the source, if the cut-off effects have been successfully removed. In both cases, but in particular at  $\beta = 6.2$ , we see a smaller deviation from the plateau at small and large  $t$  values. To obtain the mass, we fit the ratio (28) to a constant. We have used the same fit ranges as for the pion mass. The results of the fit are given in tables 10, 11. At  $\beta = 6.0$  in the improved case we see that at  $\kappa = 0.1342$  we have small finite size effects, indicating again that our results on the  $16^3 32$  lattice are not significantly volume dependent.

For both the Ward identity and the standard method we choose to determine the  $\kappa$  values from the pseudoscalar meson masses. Sometimes the  $\phi(1020)$  meson is taken for the determination of the strange quark mass. However, we do not think that this is a good idea because of potential  $\omega - \phi$  mixing [40]. We generalize eq. (8) to the case of two different quark masses by writing

$$\frac{1}{2} \left( \frac{1}{\kappa_1} + \frac{1}{\kappa_2} \right) - \frac{1}{\kappa_c} = b_2 m_{PS}^2 + b_3 m_{PS}^3 \quad (29)$$

with the same coefficients  $b_2, b_3$  as before. This is inspired by chiral perturbation theory where it is expected that the pseudoscalar mass is a function of the sum of quark and antiquark mass,  $m_q + m_{\bar{q}}$ , even when quark and antiquark have different flavors. By fixing  $m_{PS}$  to the physical pion mass  $m_{\pi^\pm}$ , using the string tension values compiled in table 8 with eq. (15) as the scale, we find the value for  $\kappa_{u,d} = \kappa_1 \equiv \kappa_2$ . The strange quark mass is obtained by identifying  $m_{PS}$  with the kaon mass  $m_{K^\pm}$ , taking  $\kappa_1 = \kappa_{u,d}$  as input and solving for  $\kappa_2 = \kappa_s$ . This gives for the light mass

$$m_{u,d} a = \frac{1}{2} \left( \frac{1}{\kappa_{u,d}} - \frac{1}{\kappa_c} \right) = \begin{cases} 0.001836(36) & \text{for } \beta = 6.0, \\ 0.001384(36) & \text{for } \beta = 6.2. \end{cases} \quad (30)$$

For the strange mass we get

$$m_s a = \frac{1}{2} \left( \frac{1}{\kappa_s} - \frac{1}{\kappa_c} \right) = \begin{cases} 0.0419(11) & \text{for } \beta = 6.0, \\ 0.0310(11) & \text{for } \beta = 6.2, \end{cases} \quad (31)$$

where  $m_{u,d} = 1/2(m_u + m_d)$ .

The bare masses  $\tilde{m}_{u,d}, \tilde{m}_s$  are computed analogously. We write

$$\tilde{m} \equiv \frac{1}{2}(\tilde{m}_1 + \tilde{m}_2) = \tilde{b}_2 m_{PS}^2 + \tilde{b}_3 m_{PS}^3. \quad (32)$$

Using this parameterization we first fit the masses in tables 10, 11 to the pseudoscalar masses in tables 2, 3. This gives us  $\tilde{b}_2, \tilde{b}_3$ . We then determine  $\tilde{m}_{u,d}, \tilde{m}_s$  by fixing  $m_{PS}$  to the physical pion and kaon masses, respectively, as before.

The mass dependence of the renormalization constant  $Z_A(am)$  can be parameterized as [41]

$$Z_A(am) = (1 + b_A am)Z_A. \quad (33)$$

The renormalization constant  $Z_A$  has been computed non-perturbatively in ref. [42]. The fit formula in this paper gives  $Z_A = 0.7924$  at  $\beta = 6.0$  and  $Z_A = 0.8089$  at  $\beta = 6.2$ . The coefficient  $b_A$  is only known perturbatively to one-loop order [43]. The best we can do at present is to take the tadpole improved value. For the boosted coupling we use  $\alpha_s^{\overline{MS}}(1/a)$ , giving

$$b_A = 1 + \alpha_s^{\overline{MS}}(1/a) 1.912, \quad (34)$$

where we take  $\alpha_s^{\overline{MS}}(1/a) = 0.1981$  at  $\beta = 6.0$  and  $\alpha_s^{\overline{MS}}(1/a) = 0.1774$  at  $\beta = 6.2$  [14]. For  $Z_P^{\overline{MS}}(a\mu, am)$  we write

$$Z_P^{\overline{MS}}(a\mu, am) = (1 + b_P am)Z_P^{\overline{MS}}(a\mu). \quad (35)$$

The renormalization constant  $Z_P^{\overline{MS}}(a\mu)$  has been computed perturbatively [44]. The result is

$$Z_P^{\overline{MS}}(a\mu) = 1 - \frac{g^2}{16\pi^2} C_F (-6 \ln(a\mu) + 22.595 - 2.249 c_{SW} + 2.036 c_{SW}^2), \quad (36)$$

with  $C_F = 4/3$ . We shall take the scale  $\mu = 1/a$  and use the tadpole improved value of eq. (36) which turns out to be

$$Z_P^{\overline{MS}}(a\mu = 1) = \left[ 1 - \frac{\alpha_s^{\overline{MS}}(1/a)}{4\pi} (16.967 - 2.999 c_{SW} u_0^3 + 2.715 (c_{SW} u_0^3)^2) \right] u_0. \quad (37)$$

(We use  $u_0 = 0.8778$  at  $\beta = 6.0$  and  $u_0 = 0.8851$  at  $\beta = 6.2$ ). The coefficient  $b_P$  has also been computed perturbatively to one-loop order [43]. Again we shall use the tadpole improved value

$$b_P = 1 + \alpha_s^{\overline{MS}}(1/a) 1.924. \quad (38)$$

We have also computed the renormalization constants  $Z_A(am)$ ,  $Z_P(a\mu, am)$  non-perturbatively [45]. So far we have results for  $\beta = 6.0$  only. Our numbers are in fair agreement with the non-perturbative calculation in ref. [42] and the tadpole improved value (37). However, for small  $\mu$  the constant  $Z_P$  behaves very differently from the perturbative formula.

To compare the results at the two different  $\beta$  values, we rescale them both to  $\mu' = 2$  GeV using formula (24). As before, we use the string tension to convert the lattice spacing into physical units. The resulting quark masses  $m_{u,d}^{\overline{MS}}(2 \text{ GeV})$ ,  $m_s^{\overline{MS}}(2 \text{ GeV})$  are given in table 12.

Let us now discuss the standard method. We already have determined  $m_{u,d}(a)$ ,  $m_s(a)$  in eqs. (30), (31). For the renormalization constant  $Z_m^{\overline{MS}}(a\mu, am)$  we write

$$Z_m^{\overline{MS}}(a\mu, am) = (1 + b_m am)Z_m^{\overline{MS}}(a\mu). \quad (39)$$

The constant  $Z_m^{\overline{MS}}(a\mu)$  has been computed perturbatively [44]. We obtain

$$Z_m^{\overline{MS}}(a\mu) = 1 - \frac{g^2}{16\pi^2} C_F (6 \ln(a\mu) - 12.952 - 7.738c_{SW} + 1.380c_{SW}^2). \quad (40)$$

The tadpole improved value, which we will be using, is

$$Z_m^{\overline{MS}}(a\mu = 1) = \left[ 1 - \frac{\alpha_s^{\overline{MS}}(1/a)}{4\pi} \left( -4.110 - 10.317c_{SW}u_0^3 + 1.840(c_{SW}u_0^3)^2 \right) \right] u_0^{-1}. \quad (41)$$

The coefficient  $b_m$  has been computed in [43]. The tadpole improved value is

$$b_m = -\frac{1}{2} - \alpha_s^{\overline{MS}}(1/a) 1.210. \quad (42)$$

Again we extrapolate the quark masses to  $\mu' = 2 \text{ GeV}$  using eq. (24). The results which follow from this approach are listed in table 12 as well.

The results of the Ward identity and the standard method may differ by  $O(a^2)$  effects, and they do. We can ‘fit’ the  $a$  dependence by

$$m_q^{\overline{MS}} = c_0 + c_2 a^2. \quad (43)$$

The result of the fit is shown in figs. 10, 11. The continuum values from this fit are given in table 12. We find that the two methods give consistent results in the continuum limit. Taking the statistical average of the two results we obtain the continuum values

$$m_{u,d}^{\overline{MS}}(2\text{GeV}) = 5.1 \pm 0.2 \text{ MeV}, \quad (44)$$

$$m_s^{\overline{MS}}(2\text{GeV}) = 112 \pm 5 \text{ MeV}. \quad (45)$$

The Ward identity method appears to have larger  $O(a^2)$  effects than the standard method.

We may compare our results with the prediction of chiral perturbation theory, which cannot give absolute values but can determine the ratio of  $m_s$  to  $m_{u,d}$ . A recent calculation gives [46]  $m_s/m_{u,d} = 24.4 \pm 1.5$ . We find  $m_s/m_{u,d} = 22.2 \pm 1.2$ .

## *Wilson Fermions*

Let us now consider the case of Wilson fermions. We proceed in the same way as before. The situation here is that  $Z_A(am)$  is known non-perturbatively only for  $\beta = 6.0$  [47], and that  $b_A$ ,  $b_P$  and  $b_m$  are only known to tree-level. So for  $Z_A$  we use the tadpole improved perturbative value

$$Z_A = \left[ 1 - \frac{\alpha_s^{\overline{MS}}(1/a)}{4\pi} 7.901 \right] u_0, \quad (46)$$

and for  $b_A$ ,  $b_P$  and  $b_m$  we take the tree-level results. Comparing  $Z_A$  with the non-perturbative determination at  $\beta = 6.0$  [47], as well as with a non-perturbative calculation at  $\beta = 5.9, 6.1$  and  $6.3$  using the Ward identity [48], we find good agreement. The renormalization constants  $Z_P^{\overline{MS}}(a\mu = 1)$  and  $Z_m^{\overline{MS}}(a\mu = 1)$  are obtained from eqs. (37), (41) by setting  $c_{SW} = 0$ . The resulting quark masses are given in table 12, and they are plotted and compared with the improved results in figs. 10, 11. In this case we expect discretization errors of  $O(a)$  instead of  $O(a^2)$ . So it is not surprising that the Ward identity and the standard method give results which are far apart. We find that the Ward identity method gives mass values which are closer to the continuum result.

Finally, in figs. 12, 13 we compare our improved quark masses with the world data of Wilson quark masses as compiled in ref. [49] for the standard method. These authors use the  $\rho$  mass extrapolated to the chiral limit to set the scale. At  $\beta = 6.0$  the scale set by the string tension and by the Wilson action  $\rho$  mass differ by about 20% which explains the difference between our Wilson data and the world data in figs. 12, 13. We see that the improved action improves the scaling behavior.

## 5 Decay Constants

The pion decay constant  $f_\pi$  is well known experimentally and can be determined from the two-point correlation functions on the lattice as well, allowing for a further test of scaling of the improved theory. We shall also look at the decay constants of the  $K$ ,  $\rho$ ,  $K^*$  and the  $a_1$  meson.

In Euclidean space at zero three-momentum we define

$$\begin{aligned}\langle 0|\mathcal{A}_4|\pi\rangle &= m_\pi f_\pi, \\ \langle 0|\mathcal{A}_i|a_1, \lambda\rangle &= e(\lambda)_i m_{a_1}^2 f_{a_1}, \\ \langle 0|\mathcal{V}_i|\rho, \lambda\rangle &= e(\lambda)_i \frac{m_\rho^2}{f_\rho},\end{aligned}\tag{47}$$

where  $\mathcal{A}$  and  $\mathcal{V}$  are the renormalized axial vector and vector current, respectively, and  $e(\lambda)$  is the polarization vector with  $\sum_\lambda e_i^*(\lambda)e_j(\lambda) = \delta_{ij}$ . The pseudoscalar and vector states are normalized by

$$\langle p|p'\rangle = (2\pi)^3 2p_0 \delta(\vec{p} - \vec{p}').\tag{48}$$

Note that our  $f_{a_1}$  is defined to be dimensionless.

In the improved theory the renormalized operators are

$$\mathcal{A}_\mu = (1 + b_A am) Z_A (A_\mu + c_A a \partial_\mu P),\tag{49}$$

$$\mathcal{V}_\mu = (1 + b_V am) Z_V (V_\mu + ic_V a \partial_\lambda T_{\mu\lambda}),\tag{50}$$

where  $V_\mu = \bar{\psi}\gamma_\mu\psi$  and  $T_{\mu\nu} = \bar{\psi}\sigma_{\mu\nu}\psi$  are the vector and tensor operators, respectively. We use the definition  $\sigma_{\mu\nu} = i[\gamma_\mu, \gamma_\nu]/2$ . Both currents are (partially) conserved, and hence no scale enters into their definition. The renormalization constant  $Z_A$  and the improvement coefficients  $c_A$  and  $b_A$  have already been given in the last section. The renormalization constant  $Z_V$  and the coefficients  $b_V$  and  $c_V$  have been computed non-perturbatively in ref. [42, 50]. At  $\beta = 6.0$  the values are  $Z_V = 0.7780$ ,  $b_V = 1.472$  and  $c_V = -0.32(6)$ , and at  $\beta = 6.2$  the numbers are  $Z_V = 0.7927$ ,  $b_V = 1.409$  and  $c_V = -0.22(7)$ . While for most of these quantities the authors have given fit formulae in  $g^2$ , for  $c_V$  we have read the numbers from the graph in [50], as no such formula exists yet. We have also determined  $Z_V$  and  $b_V$  at  $\beta = 6.0$  from our nucleon three-point functions and find consistent results.

On the lattice we extract the meson decay constant from two-point correlation functions. For large times we expect that

$$\begin{aligned} C_{\mathcal{O}_1\mathcal{O}_2}(t) &= \langle \mathcal{O}_1(t)\mathcal{O}_2^\dagger(0) \rangle \\ &= \frac{1}{2m_H} \left[ \langle 0|\mathcal{O}_1|H \rangle \langle 0|\mathcal{O}_2|H \rangle^* e^{-m_H t} + \langle 0|\mathcal{O}_1^\dagger|H \rangle^* \langle 0|\mathcal{O}_2^\dagger|H \rangle e^{-m_H(T-t)} \right] \\ &\equiv A_{\mathcal{O}_1\mathcal{O}_2} \left[ e^{-m_H t} + \eta_1\eta_2 e^{-m_H(T-t)} \right], \end{aligned} \quad (51)$$

where  $\mathcal{O}(t)$  is of the form  $V_s^{-\frac{1}{2}} \sum_{\vec{x}} \bar{\psi}(\vec{x}, t)\Gamma\psi(\vec{x}, t)$ ,  $V_s$  being the spatial volume of the lattice, and  $\mathcal{O}^\dagger = \eta\mathcal{O}$  with  $\eta = \pm 1$  being given by  $\gamma_4\Gamma^\dagger\gamma_4 = \eta\Gamma$ . The  $\eta$  factor tells us how  $\mathcal{O}$  behaves under time reversal, i.e. whether the two-point function is symmetric or antisymmetric with respect to  $t \rightarrow T - t$ . Here  $T$  is the temporal extent of the lattice. In general we have computed correlation functions with local ( $L$ ) and smeared ( $S$ ) operators.

We shall now consider the appropriate matrix elements separately. We start with those matrix elements necessary for the  $\pi$ . With our conventions we set

$$\begin{aligned} \langle 0|A_4|\pi \rangle &= m_\pi f_\pi^{(0)}, \\ \langle 0|a\partial_4 P|\pi \rangle &= -\sinh am_\pi \langle 0|P|\pi \rangle = m_\pi a f_\pi^{(1)}, \end{aligned} \quad (52)$$

where  $f^{(0)}$ ,  $f^{(1)}$  are defined to be real and positive. By computing  $C_{A_4P}^{LS}$  and  $C_{PP}^{SS}$  we find for the matrix element of  $A_4$  from eq. (52)

$$m_\pi f_\pi^{(0)} = -2\kappa \frac{\sqrt{2m_\pi} A_{A_4P}^{LS}}{\sqrt{A_{PP}^{SS}}}, \quad (53)$$

and for the matrix element of  $\partial_4 P$  we obtain from the ratio of the  $C_{PP}^{LS}$  and  $C_{A_4P}^{LS}$  correlation functions

$$\frac{a f_\pi^{(1)}}{f_\pi^{(0)}} = \sinh am_\pi \frac{A_{PP}^{LS}}{A_{A_4P}^{LS}}. \quad (54)$$

Alternatively, we can take the time derivative from the plateau in the correlation function. Numerically we found that it made very little difference to the result.

For the  $a_1$  we set

$$\langle 0|A_i|a_1, \lambda \rangle = e(\lambda)_i m_{a_1}^2 f_{a_1}^{(0)}, \quad (55)$$

and we find

$$m_{a_1}^2 f_{a_1}^{(0)} = 2\kappa \frac{\sqrt{2m_{a_1}} \sum_k A_{A_k A_k}^{LS}}{\sqrt{3} \sum_k A_{A_k A_k}^{SS}}. \quad (56)$$

For the  $\rho$  we set

$$\langle 0|V_i|\rho, \lambda \rangle = e(\lambda)_i m_\rho^2 f_\rho^{(0)}, \quad (57)$$

$$\langle 0|a\partial_4 T_{i4}|\rho, \lambda \rangle = -\sinh am_\rho \langle 0|T_{i4}|\rho, \lambda \rangle = ie(\lambda)_i m_\rho^2 a f_\rho^{(1)},$$

and we obtain

$$m_\rho^2 f_\rho^{(0)} = 2\kappa \frac{\sqrt{2m_\rho} \sum_k A_{V_k V_k}^{LS}}{\sqrt{3} \sum_k A_{V_k V_k}^{SS}} \quad (58)$$

and

$$\frac{a f_\rho^{(1)}}{f_\rho^{(0)}} = -i \sinh am_\rho \frac{\sum_k A_{T_{k4} T_{k4}}^{LS} \sqrt{\sum_k A_{V_k V_k}^{SS}}}{\sum_k A_{V_k V_k}^{LS} \sqrt{\sum_k A_{T_{k4} T_{k4}}^{SS}}}. \quad (59)$$

In tables 13 and 14 we give the lattice results for the matrix elements calculated from the above formulas. The fits to the correlation functions, as for the masses, are all made using the bootstrap method.

Collecting all the terms, the physical decay constants are given by

$$\begin{aligned} f_\pi &= (1 + b_A am) Z_A (f_\pi^{(0)} + c_A a f_\pi^{(1)}), \\ f_{a_1} &= (1 + b_A am) Z_A f_{a_1}^{(0)}, \\ 1/f_\rho &= (1 + b_V am) Z_V (f_\rho^{(0)} + c_V a f_\rho^{(1)}). \end{aligned} \quad (60)$$

When the improvement terms are weighted with the appropriate  $c$  factors, they contribute about 10-20% at  $\beta = 6.0$  and up to 10% at  $\beta = 6.2$ . It is thus important to improve the operators as well.

To perform the chiral extrapolation, we make fits similar to those for the hadron masses, namely

$$f_\pi^2 = b_0 + b_2 m_\pi^2 + b_3 m_\pi^3, \quad (61)$$

$$f_{a_1}^2 = b_0 + b_2 m_\pi^2 + b_3 m_\pi^3, \quad (62)$$

$$1/f_\rho^2 = b_0 + b_2 m_\pi^2 + b_3 m_\pi^3. \quad (63)$$



We decided to fit the square of the decay constants rather than the decay constants themselves because this shows less curvature. The fits and the data are shown in fig. 14 for  $f_\pi$  and  $f_\rho$ . We compare this result with the meson decay constants computed with the Wilson action. These follow from eq. (60) with  $c_A, c_V = 0$ . For  $Z_A$  we use the tadpole improved value given in eq. (46), and for  $b_A$  we take the tree-level result ( $b_A = 1$ ). The renormalization constant  $Z_V$  (in the chiral limit) has been determined non-perturbatively from a two-point correlation function of the local vector current [48] at  $\beta = 5.9, 6.1$  and  $6.3$ . Unlike the case of  $Z_A$ , we find significant differences between this determination and our determination using the nucleon three-point function. The latter gives  $Z_V = 0.651(15)$  at  $\beta = 6.0$  which is close to the tadpole improved result. This indicates large  $O(a)$  effects. Since we are applying  $Z_V$  to a two-point function, we chose to use the non-perturbative result from ref. [48]. We interpolate this result to  $\beta = 6.0$  and  $6.2$  and find  $Z_V = 0.565$  and  $0.618$ , respectively. For  $b_V$  we again take the tree-level result. Although the individual contributions of the improvement terms are significant, the overall result for  $f_\pi$  in fig. 14 is not much changed when compared with the Wilson case for smaller quark masses. For larger quark masses, especially at  $\beta = 6.0$ , the Wilson  $f_\pi$  is larger. The situation is different for  $f_\rho$ . Here we find a systematic difference of 10-20% at  $\beta = 6.0$  and approximately 10% at  $\beta = 6.2$  for all quark masses. In both cases the difference between the two actions becomes smaller with increasing  $\beta$  as one would expect.

Our results extrapolated to the chiral limit are given in table 15, and we compare  $f_\pi$  and  $f_\rho$  with experiment in fig. 15. For  $f_\pi$  we find reasonable agreement of the improved results with the experimental value using, as before, the string tension as the scale. When including the data of ref. [51], one sees that the Wilson results lie lower, and it appears that the values are increasing as we approach the continuum limit. For  $f_\rho$  both our improved and Wilson results lie within 5% of the experimental value. There is, however, a definite difference as we previously remarked. The Wilson numbers lie above the experimental value, while the improved ones lie below. One must remember though that in the Wilson case there is a systematic error in the renormalization constant  $Z_V$  which may be larger than the statistical errors in the figure. The experimental number for the decay constant of the  $a_1$  is [52]  $f_{a_1} = 0.17(2)$  (in our notation). The agreement between experimental and lattice values is encouraging.

We can avoid errors from extrapolating to the chiral limit by considering quark masses within our data range, as we have already done in figs. 5 and 6. The most physical  $\kappa$  values to use are those corresponding to the  $K$  mass. To obtain the decay constants we take eqs. (61) and (63) at  $m_\pi = m_K$ . (Remember that we are using  $m_\pi$  as a generic name for the pseudoscalar meson mass.) We give the results for  $f_K$  and  $f_{K^*}$  in table 15, and in fig. 16 we show the scaling behavior together with the experimental value for  $f_K$ . We find the errors to be substantially reduced. For  $f_K$  we see no difference between improved and Wilson results, both lying 10% below the experimental value. For  $f_{K^*}$  the error bars have become small enough to attempt an extrapolation to the continuum limit. The curves are a

simultaneous fit, linear for the Wilson and quadratic for the improved data, constrained to agree in the continuum limit. In this quantity there appear to be large  $O(a^2)$  effects in the improved case.

## 6 Conclusions

The goal of this paper was to investigate the scaling behavior of  $O(a)$  improved fermions. If scaling is good, the results we get should already be close to the continuum values for present values of the coupling. To this end we have done simulations for two values of  $\beta$  and looked at two-point correlation functions from which we derive hadron masses, quark masses and meson decay constants.

First we looked at hadron masses. The most visible difference between Wilson and improved fermions is that the  $\rho$  mass is much lighter in the Wilson case at comparable pion masses. In fig. 5 we see that the improved action has brought the  $\rho$  mass closer to its physical value when we use the string tension to set the scale. In this figure we have compared the Wilson action  $\rho$  masses at many different scales. We see a linear behavior in the lattice spacing  $a$  as one would expect. For improved fermions we find the discretization errors reduced for our couplings.

A problem with Wilson fermions was that they could not describe the vector-pseudoscalar mass splitting adequately. This problem seems to be cured by using improved fermions.

Quark masses are important parameters in the Standard Model. Experimentally, their values are poorly known, and a reliable lattice determination would be useful. Using two different methods, we have determined the light and strange quark masses. Our results can be seen in figs. 10, 11. Both methods give consistent results for improved fermions. In the continuum limit we find for the average of  $u$  and  $d$  quark masses  $m_{u,d}^{\overline{MS}}(2\text{ GeV}) = 5.1 \pm 0.2\text{ MeV}$  and  $m_s^{\overline{MS}}(2\text{ GeV}) = 112 \pm 5\text{ MeV}$ . In the Wilson case the discrepancy between the two methods is much larger, hinting at substantial  $O(a)$  effects.

When calculating the decay constants, an advantage of using the improved theory is that the renormalization constants and improvement coefficients for  $f_\pi$ ,  $f_{a_1}$ ,  $f_\rho$  and  $f_{K^*}$  are known. For  $f_K$  we still have to use the perturbative values of  $b_A$  because they have not yet been computed non-perturbatively. A systematic uncertainty in the Wilson case lies in the choice of the renormalization constants. While the results are in reasonable agreement with phenomenology, the data are at present not precise enough to discuss an extrapolation to the continuum limit, with the possible exception of  $f_{K^*}$ . In that case it looks that there are relatively large  $O(a^2)$  effects between  $\beta = 6.0$  and  $6.2$ .

Our general conclusion is that the Wilson action at  $\beta = 6.0$  has  $O(a)$  errors of up to 20% compared to the continuum extrapolation. The non-perturbatively  $O(a)$  improved theory still shows  $O(a^2)$  effects of up to 10% at  $\beta = 6.0$ , except for the Ward identity quark masses where the effect is somewhat larger. If one wants to go to smaller values of  $\beta$ , one probably

will have to reduce the  $O(a^2)$  errors as well. Going to  $\beta = 6.2$  reduces  $a^2$  by a factor of almost two, bringing discretization errors down to 5% or less. To achieve a one percent accuracy would require calculations at several  $\beta$  values and an extrapolation to  $a = 0$ .

## Acknowledgement

This work was supported in part by the Deutsche Forschungsgemeinschaft. The numerical calculations were performed on the Quadrics computers at DESY-Zeuthen. We wish to thank the operating staff for their support. We furthermore thank Hartmut Wittig for help with table 8 and Henning Hoerber for communicating his new string tension results to us prior to publication.

# Tables

$\beta = 5.7$							
$c_{SW} = 1.0$							
$V$	$\kappa$	$am_\pi$	$am_\rho$	$am_N$	$am_{a_0}$	$am_{a_1}$	$am_{b_1}$
16 <sup>3</sup> 32	0.1500	0.5028(17)	0.757(7)	1.135(18)	1.36(10)	1.61(19)	1.06(16)
	0.1510	0.414(2)	0.711(8)	1.040(17)	1.11(17)	1.31(12)	1.11(17)
	0.1520	0.288(5)	0.660(19)	0.92(3)	–	1.09(17)	1.25(20)
<i>c. l.</i>	0.15280(14)	0	<i>0.605(24)</i>	<i>0.797(49)</i>	–	<i>0.70(36)</i>	<i>1.31(30)</i>
$c_{SW} = 2.25$							
$V$	$\kappa$	$am_\pi$	$am_\rho$	$am_N$	$am_{a_0}$	$am_{a_1}$	$am_{b_1}$
16 <sup>3</sup> 32	0.1270	0.841(3)	1.087(8)	1.588(12)	1.64(10)	1.56(7)	1.48(13)
	0.1275	0.791(4)	1.053(10)	1.518(23)	1.56(7)	1.51(5)	1.53(9)
	0.1280	0.736(3)	1.022(11)	1.453(18)	1.50(7)	1.46(4)	1.42(7)
	0.1285	0.672(5)	0.988(9)	1.399(24)	1.57(14)	1.41(6)	1.39(7)
	0.1290	0.607(7)	0.955(8)	1.320(20)	1.59(14)	1.34(8)	1.33(11)
	0.1295	0.519(11)	0.922(16)	1.23(3)	–	1.28(10)	1.33(16)
<i>c. l.</i>	0.13074(29)	0	<i>0.793(19)</i>	<i>0.948(46)</i>	<i>1.43(33)</i>	<i>1.06(16)</i>	<i>1.13(25)</i>

Table 1: Hadron masses at  $\beta = 5.7$  for Sheikholeslami-Wohlert fermions with  $c_{SW} = 1$  and 2.25. In the bottom row we give  $\kappa_c$  and the mass values extrapolated to the chiral limit. The numbers in roman (*italic*) are from three-parameter (two-parameter) fits. The errors are bootstrap errors.

$\beta = 6.0$							
$c_{SW} = 0$							
$V$	$\kappa$	$am_\pi$	$am_\rho$	$am_N$	$am_{a_0}$	$am_{a_1}$	$am_{b_1}$
$16^3 32$	0.1487	0.6384(18)	0.683(2)	1.071(7)	0.885(19)	0.933(13)	0.940(19)
	0.1515	0.5037(8)	0.5696(10)	0.9019(17)	0.817(7)	0.851(7)	0.849(13)
	0.1530	0.4237(8)	0.5080(11)	0.7977(20)	0.763(11)	0.797(6)	0.809(7)
	0.1550	0.3009(10)	0.4264(14)	0.6517(30)	0.735(15)	0.717(12)	0.736(9)
$24^3 32$	0.1550	0.292(2)	0.418(5)	0.638(8)	0.610(48)	0.657(33)	0.659(35)
	0.1558	0.229(2)	0.384(7)	0.555(12)	0.616(90)	0.613(41)	0.638(38)
	0.1563	0.179(3)	0.358(11)	0.488(22)	0.88(15)	0.584(52)	0.615(44)
<i>c. l.</i>	0.15713(3)	0	0.327(6)	0.412(16)	<i>0.658(19)</i>	<i>0.632(14)</i>	<i>0.650(13)</i>
$c_{SW} = 1.769$							
$V$	$\kappa$	$am_\pi$	$am_\rho$	$am_N$	$am_{a_0}$	$am_{a_1}$	$am_{b_1}$
$16^3 32$	0.1300	0.707(2)	0.783(6)	1.190(6)			
	0.1310	0.627(2)	0.714(3)	1.079(7)			
	0.1320	0.545(5)	0.644(8)	0.974(16)			
	0.1324	0.5039(7)	0.6157(16)	0.932(4)	0.779(14)	0.829(12)	0.853(7)
	0.1333	0.4122(8)	0.5502(23)	0.821(5)	0.738(15)	0.773(7)	0.799(10)
	0.1342	0.2988(17)	0.487(3)	0.705(9)	0.92(5)	0.68(2)	0.775(15)
$24^3 32$	0.1342	0.3020(11)	0.491(3)	0.686(7)	0.82(3)	0.715(19)	0.758(16)
	0.1346	0.2388(14)	0.467(6)	0.626(10)	1.00(8)	0.684(26)	0.745(20)
	0.1348	0.194(4)	0.448(13)	0.593(19)	1.52(20)	0.664(34)	0.736(29)
<i>c. l.</i>	0.13531(1)	0	0.417(7)	0.511(15)	<i>0.816(33)</i>	<i>0.625(19)</i>	<i>0.710(14)</i>

Table 2: Hadron masses at  $\beta = 6.0$  for Wilson fermions ( $c_{SW} = 0$ ) and improved fermions ( $c_{SW} = 1.769$ ). Otherwise the notation is the same as in table 1.

$\beta = 6.2$							
$c_{SW} = 0$							
$V$	$\kappa$	$am_\pi$	$am_\rho$	$am_N$	$am_{a_0}$	$am_{a_1}$	$am_{b_1}$
24 <sup>3</sup> 48	0.1468	0.5258(12)	0.5585(16)	0.872(5)	0.685(8)	0.700(21)	0.695(21)
	0.1489	0.4148(13)	0.4615(19)	0.720(6)	0.589(8)	0.624(9)	0.626(9)
	0.1509	0.2947(14)	0.3672(27)	0.560(10)	0.507(14)	0.536(13)	0.540(13)
	0.1518	0.2299(15)	0.326(4)	0.487(12)	0.474(20)	0.509(16)	0.519(17)
	0.1523	0.1867(17)	0.307(6)	0.448(14)	0.479(30)	0.492(17)	0.511(21)
<i>c. l.</i>	0.15336(4)	0	0.255(9)	0.342(28)	0.407(17)	0.449(15)	0.464(16)
$c_{SW} = 1.614$							
$V$	$\kappa$	$am_\pi$	$am_\rho$	$am_N$	$am_{a_0}$	$am_{a_1}$	$am_{b_1}$
24 <sup>3</sup> 48	0.1321	0.5179(7)	0.5738(11)	0.877(4)	0.691(5)	0.723(6)	0.727(6)
	0.1333	0.4143(8)	0.4850(15)	0.735(5)	0.603(10)	0.642(5)	0.638(8)
	0.1344	0.3046(9)	0.4005(26)	0.592(9)	0.532(21)	0.563(7)	0.566(9)
	0.1349	0.2444(9)	0.3626(43)	0.521(13)	0.543(22)	0.529(10)	0.539(12)
	0.1352	0.2016(11)	0.3430(53)	0.485(6)	0.646(53)	0.514(13)	0.523(25)
<i>c. l.</i>	0.13589(2)	0	0.287(9)	0.378(18)	0.460(21)	0.460(9)	0.465(12)

Table 3: Hadron masses at  $\beta = 6.2$  for Wilson fermions ( $c_{SW} = 0$ ) and improved fermions ( $c_{SW} = 1.614$ ). Otherwise the notation is the same as in table 1.

$\beta$	$c_{SW}$	eq. (6)		eq. (7)		eq. (8)	
		$\kappa_c$	$\chi^2/\text{dof}$	$\kappa_c$	$\chi^2/\text{dof}$	$\kappa_c$	$\chi^2/\text{dof}$
5.7	1.0	0.15305(5)	3.0	0.15274(15)	-	0.15280(14)	-
	2.25	0.13120(7)	0.7	0.13065(28)	0.1	0.13074(29)	0.1
6.0	0	0.15695(1)	17.5	0.15726(5)	8.6	0.15713(3)	6.6
	1.769	0.13521(1)	11.5	0.13537(2)	1.5	0.13531(1)	1.0
6.2	0	0.15308(1)	30.8	0.15361(8)	0.7	0.15336(4)	0.0
	1.614	0.13574(1)	39.6	0.13601(3)	1.2	0.13589(2)	0.1

Table 4: The critical values of  $\kappa$ ,  $\kappa_c$ , of our data for the linear (eq. (6)), chiral (eq. (7)) and phenomenological fit (eq. (8)) for the various  $c_{SW}$  parameters.

$\beta$	$\kappa$	$am_\pi$	$am_\rho$	$am_N$	Lattice	Reference
6.30	0.1400	0.789(4)	0.804(4)		$32^3 \times 48$	[16]
6.30	0.1430	0.646(6)	0.670(5)		$32^3 \times 48$	[16]
6.30	0.1460	0.4879(12)	0.5188(18)	0.8252(42)	$24^3 \times 32$	[17]
6.30	0.1480	0.382(4)	0.429(4)		$32^3 \times 48$	[16]
6.30	0.1485	0.3480(14)	0.3990(23)	0.6340(47)	$24^3 \times 32$	[17]
6.30	0.1498	0.2631(19)	0.3354(30)	0.5215(67)	$24^3 \times 32$	[17]
6.30	0.1500	0.253(6)	0.333(4)		$32^3 \times 48$	[16]
6.30	0.1505	0.2093(26)	0.3012(40)	0.4506(89)	$24^3 \times 32$	[17]
6.20	0.1468	0.5258(12)	0.5585(16)	0.872(5)	$24^3 \times 48$	this work
6.20	0.1489	0.4148(13)	0.4615(19)	0.720(6)	$24^3 \times 48$	this work
6.20	0.1509	0.2947(14)	0.3672(27)	0.560(10)	$24^3 \times 48$	this work
6.20	0.1510	0.289(1)	0.366(2)	0.566(4)	$24^3 \times 64$	[18]
6.20	0.1515	0.254(1)	0.343(3)	0.525(6)	$24^3 \times 64$	[18]
6.20	0.1518	0.2299(15)	0.326(4)	0.487(12)	$24^3 \times 48$	this work
6.20	0.1520	0.220(7)	0.327(9)	0.495(10)	$24^3 \times 48$	[19]
6.20	0.1520	0.215(1)	0.321(5)	0.48(1)	$24^3 \times 64$	[18]
6.20	0.1523	0.1867(17)	0.307(6)	0.448(14)	$24^3 \times 48$	this work
6.20	0.1526	0.158(1)	0.29(1)	0.45(3)	$24^3 \times 64$	[18]
6.17	0.1500	0.3866(12)	0.4458(18)	0.6966(40)	$32^2 \times 30 \times 40$	[20]
6.17	0.1519	0.2631(12)	0.3572(26)	0.5460(52)	$32^2 \times 30 \times 40$	[20]
6.17	0.1526	0.2064(15)	0.3245(39)	0.4848(68)	$32^2 \times 30 \times 40$	[20]
6.17	0.1532	0.1455(20)	0.2965(88)	0.4097(78)	$32^2 \times 30 \times 40$	[20]

Table 5: World Wilson fermion masses above  $\beta = 6.0$ .

$\beta$	$\kappa$	$am_\pi$	$am_\rho$	$am_N$	Lattice	Reference
6.0	0.1450	0.8069(7)	0.8370(9)	1.3225(28)	$24^3 \times 54$	[21]
6.0	0.1487	0.6384(18)	0.683(2)	1.071(7)	$16^3 \times 32$	this work
6.0	0.1515	0.5037(8)	0.5696(10)	0.9019(17)	$16^3 \times 32$	this work
6.0	0.1520	0.4772(9)	0.5486(15)	0.8669(49)	$24^3 \times 54$	[21]
6.0	0.1520	0.474(1)	0.545(2)	0.861(5)	$18^3 \times 32$	[17]
6.0	0.1530	0.423(1)	0.508(3)	0.801(6)	$18^3 \times 64$	[18]
6.0	0.1530	0.4237(8)	0.5080(11)	0.7977(20)	$16^3 \times 32$	this work
6.0	0.1530	0.422(1)	0.505(1)	0.786(3)	$32^3 \times 64$	[22]
6.0	0.1540	0.364(1)	0.468(4)	0.729(7)	$18^3 \times 64$	[18]
6.0	0.1545	0.33076(28)	0.4425(10)	0.6777(21)	$24^3 \times 64$	[23]
6.0	0.1550	0.298(1)	0.431(6)	0.66(1)	$18^3 \times 64$	[18]
6.0	0.1550	0.3009(10)	0.4264(14)	0.6517(30)	$16^3 \times 32$	this work
6.0	0.1550	0.29642(27)	0.4220(12)	0.6393(27)	$24^3 \times 64$	[23]
6.0	0.1550	0.292(2)	0.418(5)	0.638(8)	$24^3 \times 32$	this work
6.0	0.1550	0.2967(15)	0.4218(42)	0.6440(85)	$24^3 \times 54$	[21]
6.0	0.1550	0.296(1)	0.422(2)	0.630(5)	$32^3 \times 64$	[22]
6.0	0.1555	0.25864(33)	0.4016(17)	0.6003(37)	$24^3 \times 64$	[23]
6.0	0.1555	0.2588(16)	0.3982(61)	0.6007(109)	$24^3 \times 54$	[21]
6.0	0.1558	0.234(1)	0.387(3)	0.557(7)	$32^3 \times 64$	[22]
6.0	0.1558	0.229(2)	0.384(7)	0.555(12)	$24^3 \times 32$	this work
6.0	0.1563	0.1847(27)	0.353(15)	0.536(30)	$24^3 \times 54$	[21]
6.0	0.1563	0.185(1)	0.361(5)	0.506(11)	$32^3 \times 64$	[22]
6.0	0.1563	0.179(3)	0.358(11)	0.488(22)	$24^3 \times 32$	this work

Table 6: World Wilson fermion masses at  $\beta = 6.0$ .



$\beta$	$\kappa$	$am_\pi$	$am_\rho$	$am_N$	Lattice	Reference
5.93	0.1543	0.4572(26)	0.5527(40)	0.8674(102)	$24^3 \times 36$	[20]
5.93	0.1560	0.3573(19)	0.4864(42)	0.7448(99)	$24^3 \times 36$	[20]
5.93	0.1573	0.2641(25)	0.4369(48)	0.6423(80)	$24^3 \times 36$	[20]
5.93	0.1581	0.1885(31)	0.4071(57)	0.5652(92)	$24^3 \times 36$	[20]
5.85	0.1440	1.0293(12)	1.0598(15)	1.6961(50)	$24^3 \times 54$	[21]
5.85	0.1540	0.6122(11)	0.6931(27)	1.1060(55)	$24^3 \times 54$	[21]
5.85	0.1585	0.3761(12)	0.5294(69)	0.815(13)	$24^3 \times 54$	[21]
5.85	0.1585	0.378(2)	0.530(6)	0.783(10)	$16^3 \times 32$	[24]
5.85	0.1595	0.3088(14)	0.4856(96)	0.744(17)	$24^3 \times 54$	[21]
5.85	0.1600	0.2730(30)	0.486(9)	0.673(9)	$16^3 \times 32$	[24]
5.85	0.1605	0.2226(21)	0.434(20)	0.683(48)	$24^3 \times 54$	[21]
5.70	0.1600	0.6905(31)	0.8022(56)	1.3124(135)	$24^3 \times 32$	[20]
5.70	0.1600	0.6873(24)	0.8021(29)	1.2900(60)	$16^3 \times 20$	[25]
5.70	0.1610	0.6527(15)	0.7842(26)	1.263(5)	$12^3 \times 24$	[17]
5.70	0.1630	0.5621(18)	0.7232(35)	1.153(6)	$12^3 \times 24$	[17]
5.70	0.1640	0.5080(29)	0.6822(38)	1.0738(80)	$16^3 \times 20$	[25]
5.70	0.1650	0.4604(22)	0.6663(45)	1.039(8)	$12^3 \times 24$	[17]
5.70	0.1650	0.4589(22)	0.6491(73)	1.0301(104)	$24^3 \times 32$	[20]
5.70	0.1663	0.3829(26)	0.6206(103)	0.9421(131)	$24^3 \times 32$	[20]
5.70	0.1665	0.3674(39)	0.6085(58)	0.915(11)	$16^3 \times 20$	[25]
5.70	0.1670	0.3302(30)	0.6042(83)	0.919(14)	$12^3 \times 24$	[17]
5.70	0.1675	0.2955(24)	0.5912(125)	0.8668(177)	$24^3 \times 32$	[20]

Table 7: World Wilson fermion masses below  $\beta = 6.0$ .

$\beta$	$a\sqrt{K}$	Reference	$r_0/a$	Reference	$r_0\sqrt{K}$
6.8	0.0730(12)	[29]	16.7(4)	[15]	1.22(4)
6.5	0.1068(10)	[30]			
6.4	0.1215(12)	[29]	9.87(8)	[15]	1.197(15)
	0.1218(28)	[31]	9.70(24)	[31]	
	0.1215(11)	Combined	9.85(8)	Combined	
6.3	0.1394(11)	Interpolated			
6.2	0.1610(9)	[32]	7.36(4)	[15]	1.185(9)
	0.1608(23)	[31]	7.33(25)	[31]	
	0.1609(28)	[33]			
	0.1610(8)	Combined	7.36(4)	Combined	
6.17	0.1677(8)	Interpolated			
6.0	0.2209(23)	[32]	5.28(4)	[15]	1.161(12)
	0.2154(50)	[31]	5.53(15)	[31]	
	0.2182(21)	[34]			
	0.2191(15)	Combined	5.30(4)	Combined	
5.93	0.2536(29)	Interpolated			
5.90	0.2702(37)	[35]	4.62(11)	[15]	1.25(3)
5.85	0.2986(27)	Interpolated			
5.8	0.3302(30)	[35]	3.63(5)	[15]	1.199(20)
5.7	0.4099(24)	[35]	2.86(5)	[15]	1.172(22)
5.6			2.29(6)	[15]	
5.5			2.01(3)	[15]	

Table 8: The lattice spacing expressed in terms of the string tension  $K$  and the force parameter  $r_0$ . When several groups have computed these quantities, we have taken the weighted average, while we interpolate logarithmically whenever the values are not known.

$\beta$	$\kappa_c$
6.40	0.150759(145)
6.30	0.151774(36)
6.20	0.153374(17)
6.17	0.153838(37)
6.00	0.157211(8)
5.93	0.158985(73)
5.85	0.161716(23)
5.70	0.169313(72)

Table 9: The critical values of  $\kappa$ ,  $\kappa_c$ , for the Wilson world data.

$\beta = 6.0$		
$c_{SW} = 0$		
$V$	$\kappa$	$2a\tilde{m}$
$16^3 32$	0.1487	0.2959(5)
	0.1515	0.1866(5)
	0.1530	0.1321(5)
	0.1550	0.0642(7)
$c_{SW} = 1.769$		
$V$	$\kappa$	$2a\tilde{m}$
$16^3 32$	0.1300	0.2836(3)
	0.1310	0.2279(3)
	0.1324	0.15231(10)
	0.1333	0.10380(11)
	0.1342	0.0553(2)
$24^3 32$	0.1342	0.0551(3)
	0.1346	0.0330(3)
	0.1348	0.0214(4)

Table 10: The bare quark masses  $\tilde{m}$  for Wilson fermions ( $c_{SW} = 0$ ) and improved fermions ( $c_{SW} = 1.769$ ) at  $\beta = 6.0$ . The errors are bootstrap errors.

$\beta = 6.2$		
$c_{SW} = 0$		
$V$	$\kappa$	$2a\tilde{m}$
24 <sup>3</sup> 48	0.1468	0.2474(3)
	0.1489	0.1616(3)
	0.1509	0.0845(3)
	0.1518	0.0514(3)
	0.1523	0.0336(3)
$c_{SW} = 1.614$		
$V$	$\kappa$	$2a\tilde{m}$
24 <sup>3</sup> 48	0.1321	0.2161887)
	0.1333	0.14585(7)
	0.1344	0.08185(7)
	0.1349	0.05283(8)
	0.1352	0.03538(9)

Table 11: The bare quark masses  $\tilde{m}$  for Wilson fermions ( $c_{SW} = 0$ ) and improved fermions ( $c_{SW} = 1.614$ ) at  $\beta = 6.0$ . The errors are bootstrap errors.

$\beta$	$c_{SW}$	$m_{u,d}^{\overline{MS}}$		$m_s^{\overline{MS}}$	
		Ward	Standard	Ward	Standard
6.0	0	$4.40 \pm 0.17$	$6.47 \pm 0.20$	$105.0 \pm 4.5$	$141.8 \pm 6.0$
6.2	0	$4.73 \pm 0.14$	$6.39 \pm 0.25$	$108.5 \pm 4.2$	$138.8 \pm 7.4$
6.0	1.769	$4.02 \pm 0.10$	$4.94 \pm 0.93$	$92.8 \pm 2.9$	$109.4 \pm 3.9$
6.2	1.614	$4.47 \pm 0.06$	$5.09 \pm 0.16$	$101.6 \pm 1.7$	$111.7 \pm 4.7$
$\infty$		$5.00 \pm 0.18$	$5.27 \pm 0.36$	$111.9 \pm 5.0$	$114.4 \pm 11.1$

Table 12: Our results of the renormalized quark masses  $m^{\overline{MS}}(2 \text{ GeV})$  in MeV for improved and Wilson fermions, together with the extrapolation to the continuum limit ( $\beta = \infty$ ). The continuum numbers refer to improved fermions. We give the results for both the Ward identity and the standard method.

$\beta = 6.0$						
$c_{SW} = 0$						
$V$	$\kappa$	$af_{\pi}^{(0)}$	–	$f_{\rho}^{(0)}$	–	$f_{a_1}^{(0)}$
16 <sup>3</sup> 32	0.1487	0.136(2)		0.305(5)		0.161(5)
	0.1515	0.122(2)		0.364(5)		0.207(3)
	0.1530	0.113(2)		0.397(7)		0.231(3)
	0.1550	0.098(2)		0.459(9)		0.262(4)
$c_{SW} = 1.769$						
$V$	$\kappa$	$af_{\pi}^{(0)}$	$af_{\pi}^{(1)}/f_{\pi}^{(0)}$	$f_{\rho}^{(0)}$	$af_{\rho}^{(1)}/f_{\rho}^{(0)}$	$f_{a_1}^{(0)}$
16 <sup>3</sup> 32	0.1300	0.1341(15)	1.792(7)	0.209(9)	0.670(2)	0.131(7)
	0.1310	0.1295(15)	1.698(8)	0.228(3)	0.588(2)	0.153(13)
	0.1324	0.1204(8)	1.599(5)	0.261(2)	0.4823(12)	0.172(7)
	0.1333	0.1128(9)	1.541(3)	0.288(3)	0.4147(15)	0.202(16)
	0.1342	0.1037(8)	1.511(6)	0.323(3)	0.353(2)	0.208(16)
24 <sup>3</sup> 32	0.1342	0.105(2)	1.521(16)	0.330(7)	0.348(3)	0.212(10)
	0.1346	0.101(2)	1.58(3)	0.352(7)	0.327(6)	0.225(14)
	0.1348	0.100(3)	1.62(5)	0.352(15)	0.324(19)	0.25(2)

Table 13: The various contributions to the decay constants  $f_{\pi}$ ,  $f_{\rho}$  and  $f_{a_1}$  at  $\beta = 6.0$ .

$\beta = 6.2$						
$c_{SW} = 0$						
$V$	$\kappa$	$af_{\pi}^{(0)}$	—	$f_{\rho}^{(0)}$	—	$f_{a_1}^{(0)}$
24 <sup>3</sup> 48	0.1468	0.1025(19)		0.268(5)		0.127(9)
	0.1489	0.0930(17)		0.315(6)		0.180(4)
	0.1509	0.0798(14)		0.376(7)		0.230(4)
	0.1518	0.0719(13)		0.412(9)		0.261(4)
	0.1523	0.0669(14)		0.438(10)		0.276(5)
$c_{SW} = 1.614$						
$V$	$\kappa$	$af_{\pi}^{(0)}$	$af_{\pi}^{(1)}/f_{\pi}^{(0)}$	$f_{\rho}^{(0)}$	$af_{\rho}^{(1)}/f_{\rho}^{(0)}$	$f_{a_1}^{(0)}$
24 <sup>3</sup> 48	0.1321	0.0985(11)	1.297(3)	0.211(3)	0.4637(8)	0.133(2)
	0.1333	0.0913(11)	1.198(4)	0.243(3)	0.3719(10)	0.167(2)
	0.1344	0.0818(10)	1.133(2)	0.283(4)	0.2900(15)	0.204(3)
	0.1349	0.0758(9)	1.118(7)	0.308(5)	0.255(2)	0.226(3)
	0.1352	0.072(3)	1.131(11)	0.327(16)	0.235(4)	0.241(11)

Table 14: The same as table 13 but for  $\beta = 6.2$ .

$\beta$	$c_{SW}$	$af_{\pi}$	$f_{a_1}$	$1/f_{\rho}$	$af_K$	$1/f_{K^*}$
6.0	0	0.0569(77)	0.2240(76)	0.295(11)	0.0732(26)	0.2385(24)
6.2	0	0.0423(36)	0.2429(48)	0.2971(71)	0.0537(11)	0.2345(28)
6.0	1.769	0.0627(20)	0.195(10)	0.2664(39)	0.0721(8)	0.2020(13)
6.2	1.614	0.0462(38)	0.2130(45)	0.2726(74)	0.0557(14)	0.2149(19)

Table 15: The decay constants  $f_{\pi}$ ,  $f_{a_1}$ ,  $f_{\rho}$  extrapolated to the chiral limit, as well as  $f_K$ ,  $f_{K^*}$  taken at the physical quark mass.

# Figures

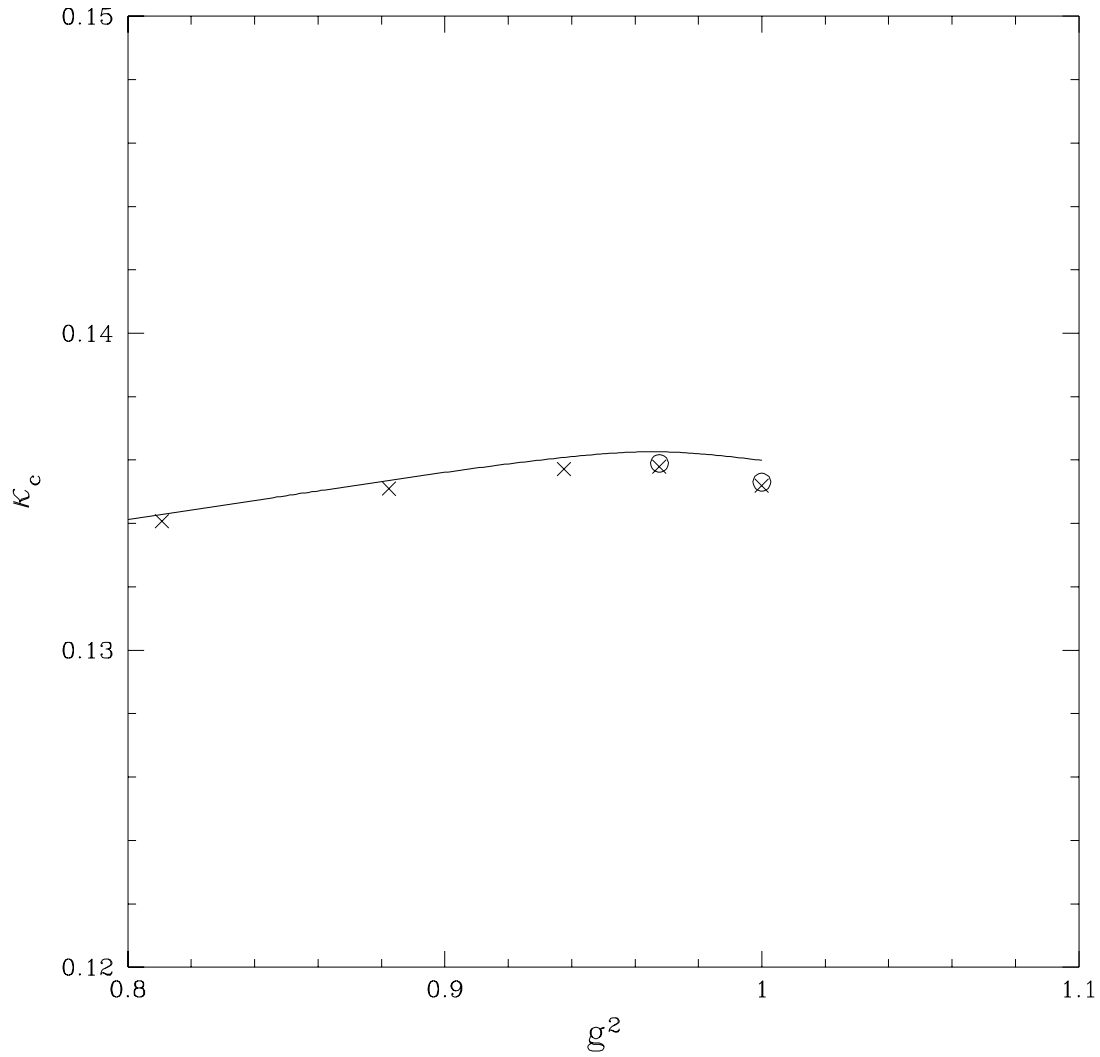


Figure 1: The critical values of  $\kappa$  for improved Wilson fermions as a function of  $g^2$  from this work ( $\circ$ ) and ref. [4] ( $\times$ ). The curve is the tadpole improved result given in eq. (10).

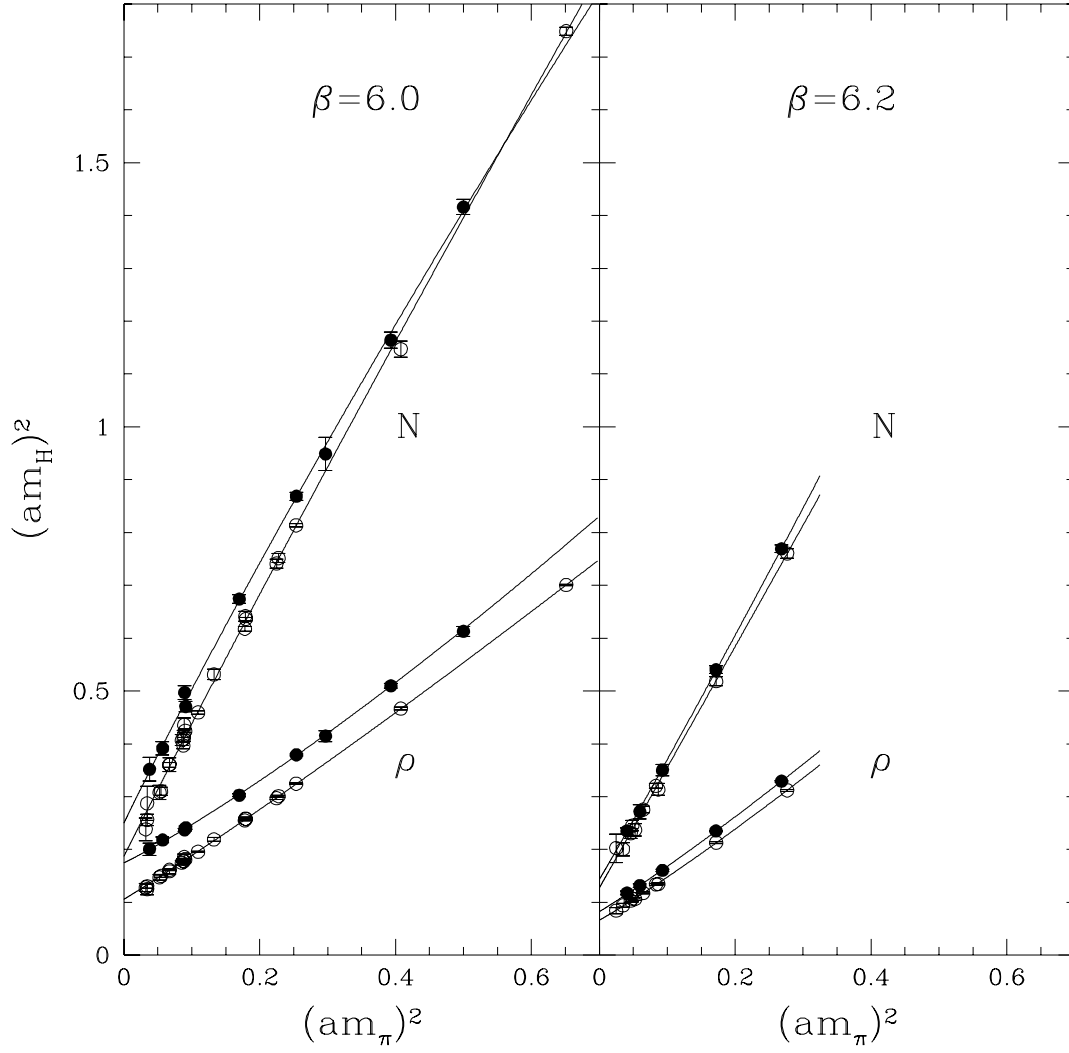


Figure 2: Fits and chiral extrapolations of  $\rho$  and nucleon masses for improved ( $\bullet$ ) and Wilson fermions ( $\circ$ ).



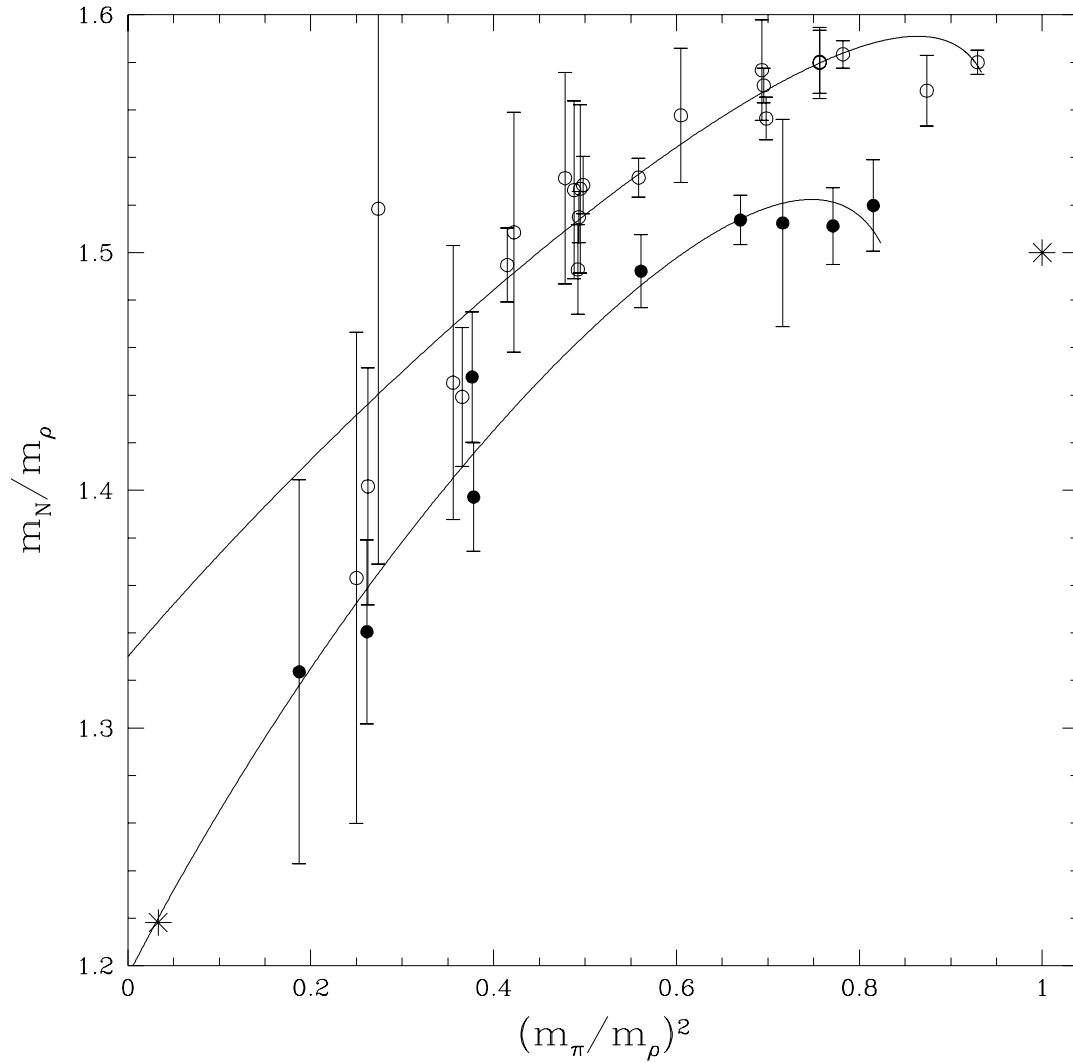


Figure 3: *APE* plot at  $\beta = 6.0$  for improved ( $\bullet$ ) and Wilson fermions ( $\circ$ ) compared with the physical mass ratio ( $*$ ) at the physical quark mass and in the heavy quark limit. The solid lines are from the mass fits described in the text.

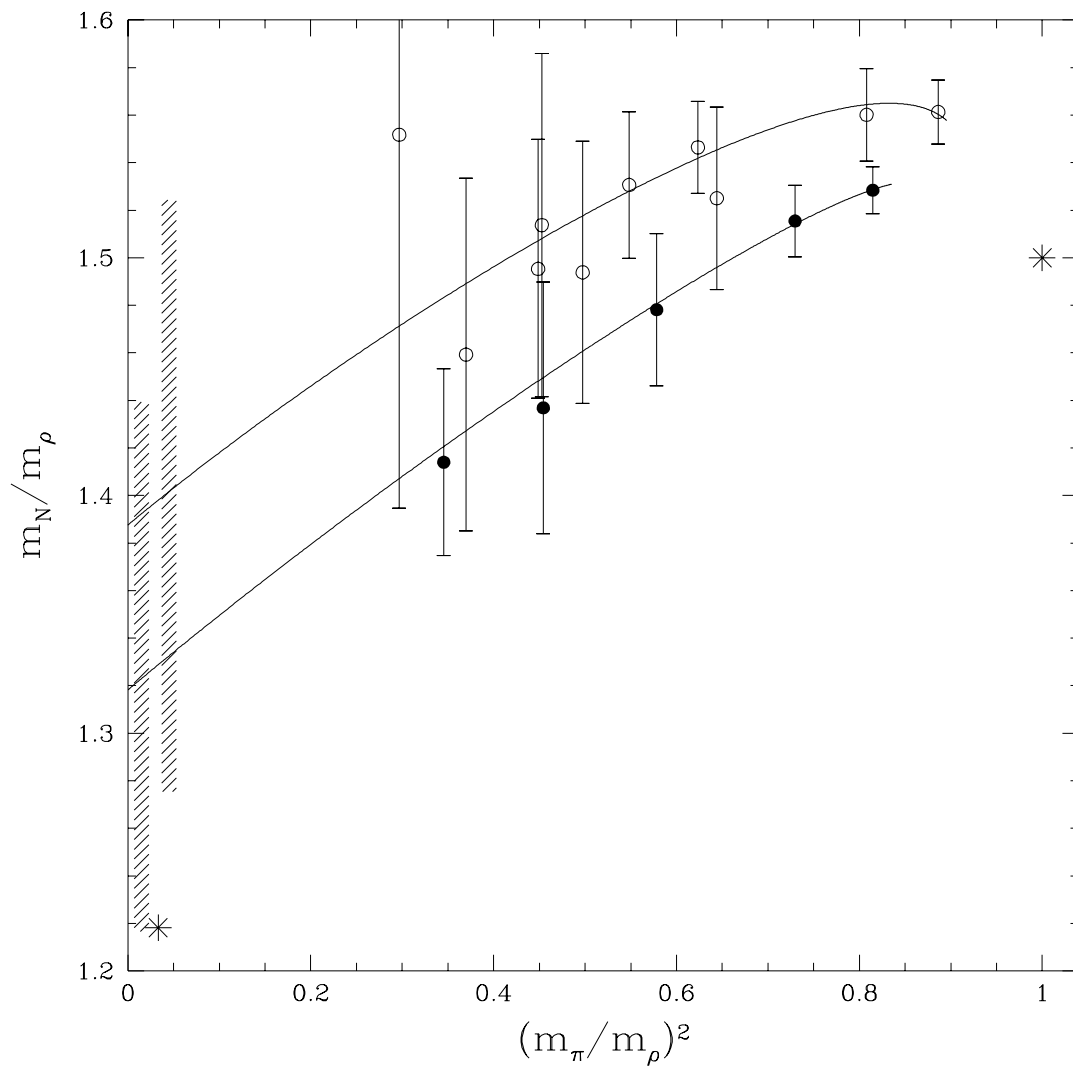


Figure 4: The same as fig. 3, but for  $\beta = 6.2$ . The hatched bars indicate the errors in the chiral limit.

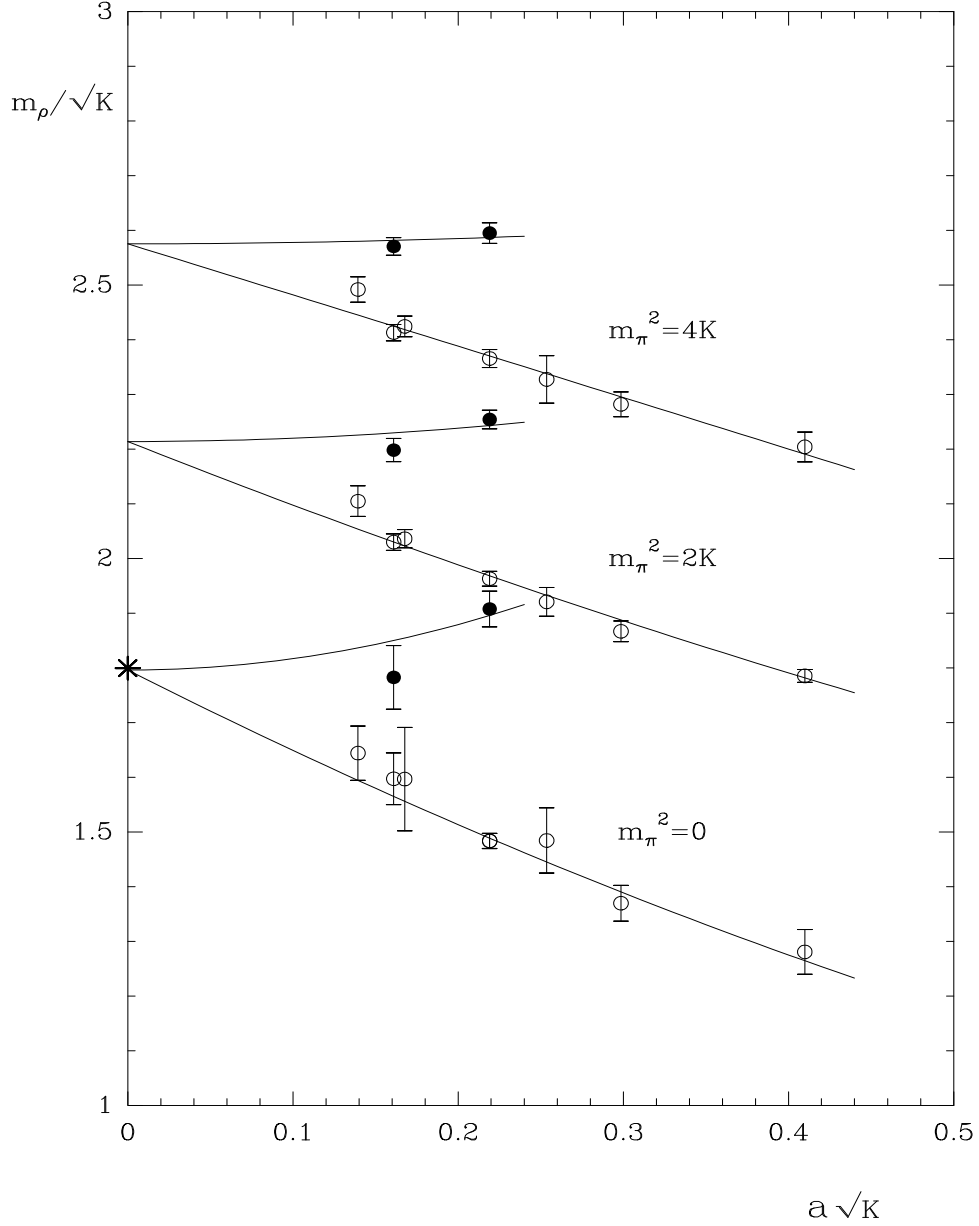


Figure 5: The ratio  $m_\rho/\sqrt{K}$  as a function of the lattice spacing for improved ( $\bullet$ ) and Wilson fermions ( $\circ$ ). The solid lines are from a simultaneous linear plus quadratic fit to the Wilson data and a quadratic fit to the improved data. This is compared with the experimental value ( $*$ ) using  $\sqrt{K} = 427$  MeV.

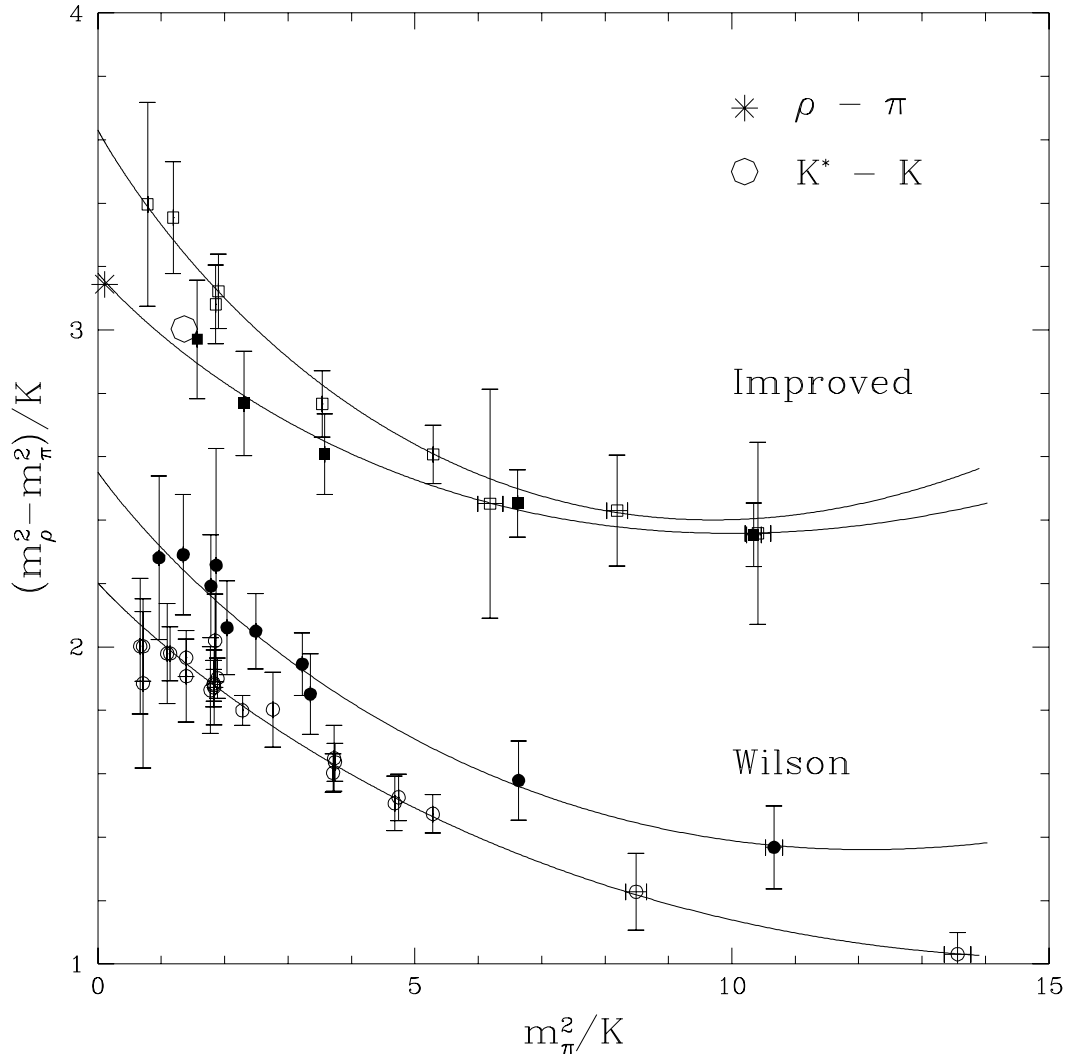


Figure 6: The vector-pseudoscalar mass splitting as a function of the quark mass. Open symbols correspond to  $\beta = 6.0$ , solid symbols to  $\beta = 6.2$ . This is compared with the physical  $\rho$ - $\pi$  (\*) and  $K^*$ - $K$  (octagon) mass splitting. The curves are from the mass fits.

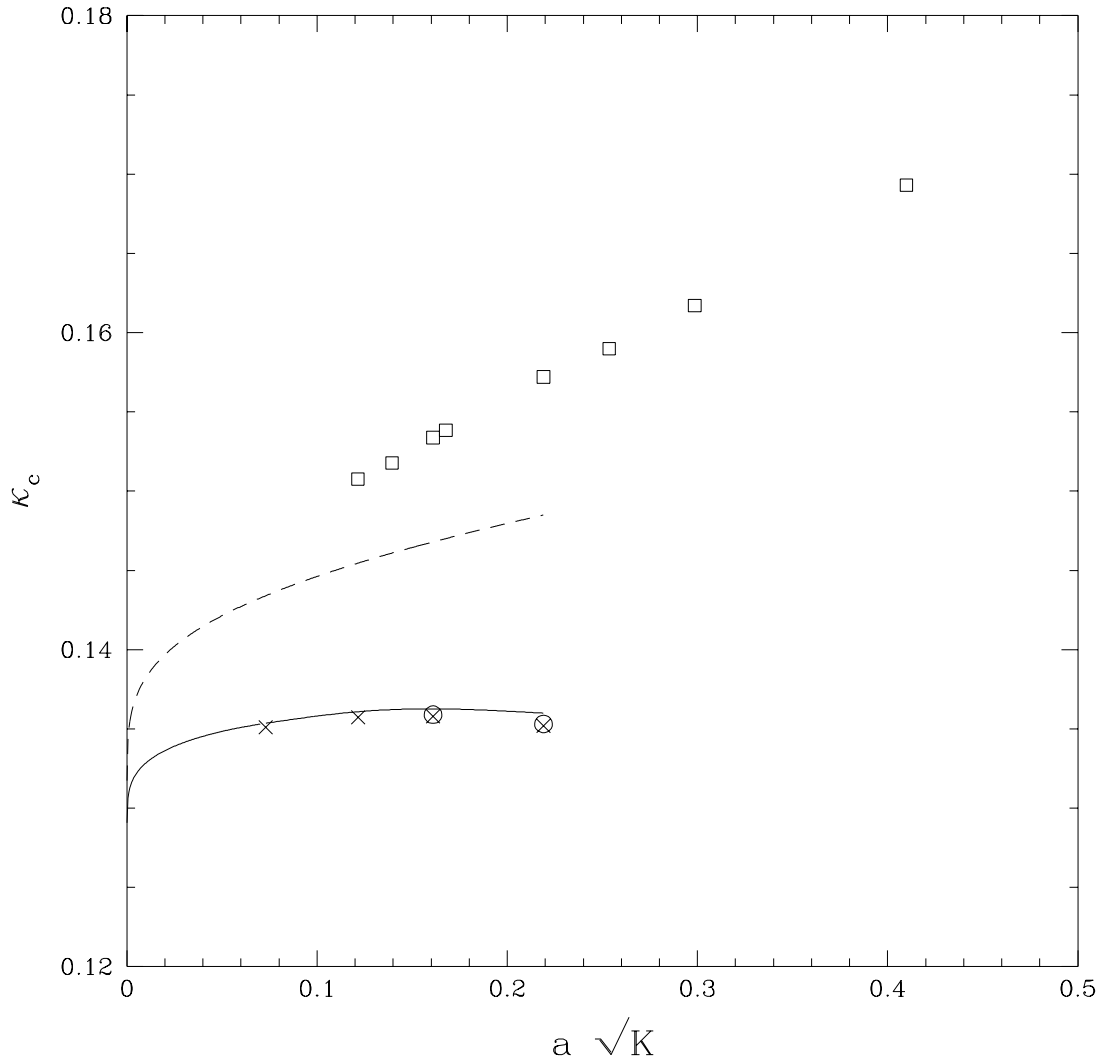


Figure 7: The critical value of  $\kappa$  as a function of the lattice spacing for Wilson fermions ( $\square$ ). The dashed curve is the prediction of tadpole improved perturbation theory. This is compared with the results for improved fermions from fig. 1.

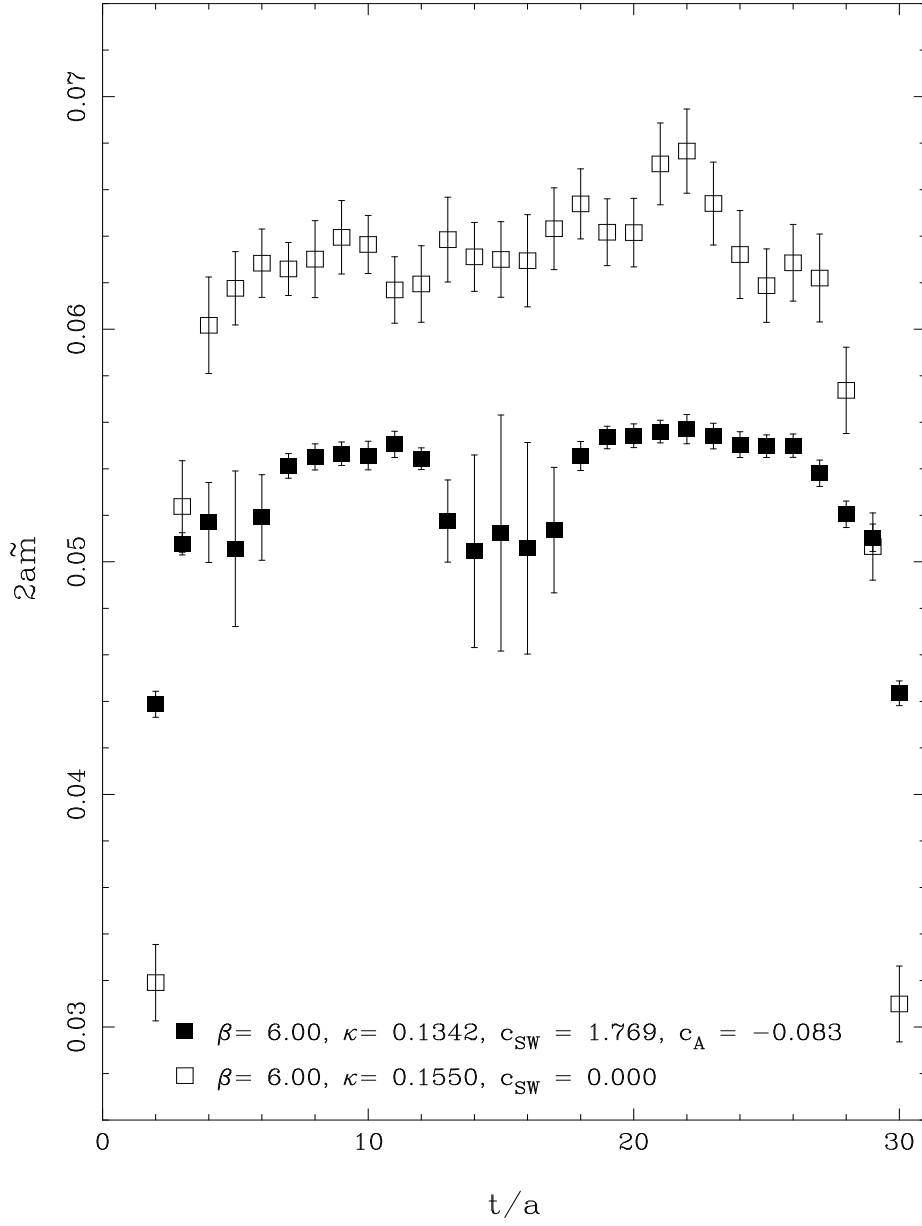


Figure 8: The bare mass  $\tilde{m}$  from the Ward identity method at  $\beta = 6.0$  for Wilson ( $\square$ ) and improved fermions ( $\blacksquare$ ) on the  $16^3 32$  lattice. The errors are bootstrap errors.

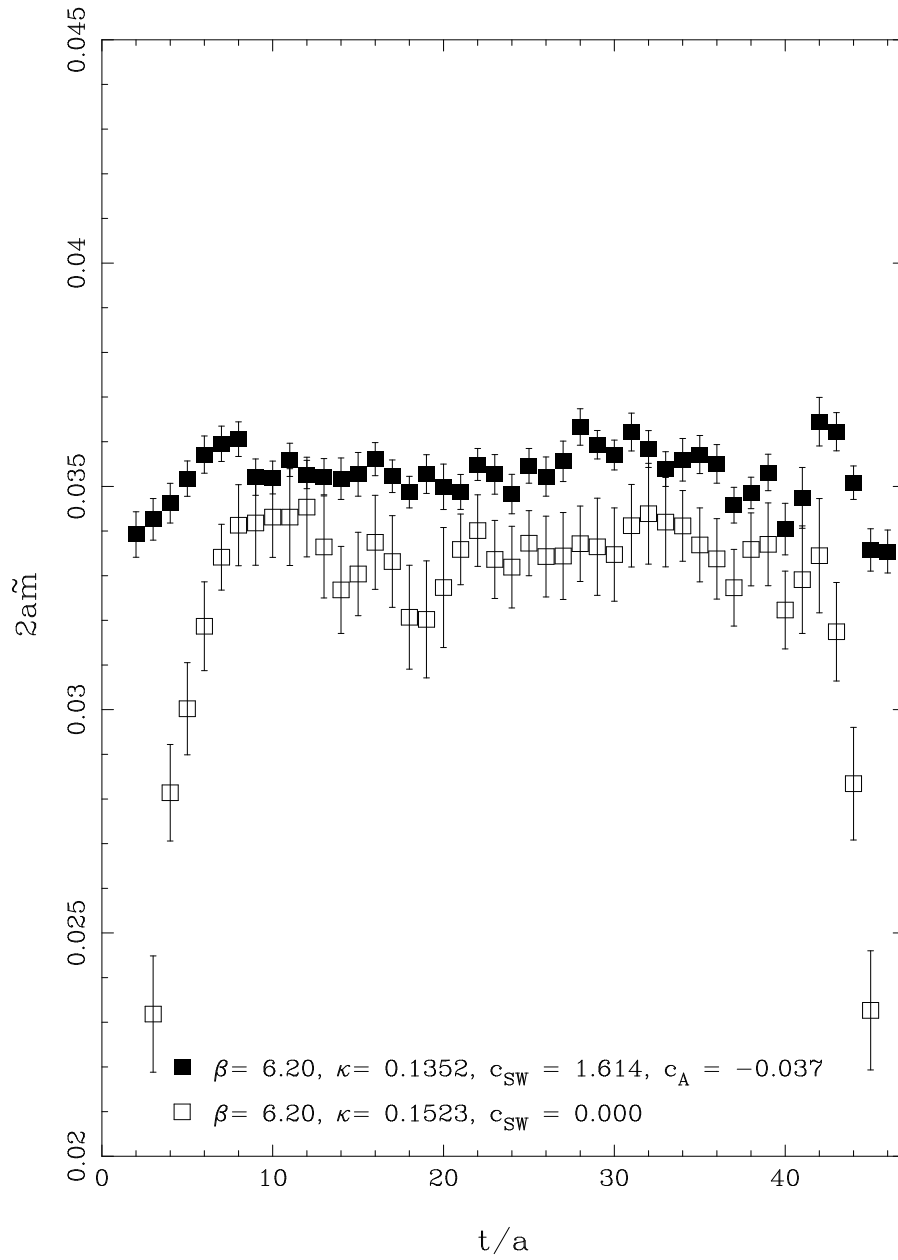


Figure 9: The same as fig. 8 but for  $\beta = 6.2$  for Wilson ( $\square$ ) and improved fermions ( $\blacksquare$ ).

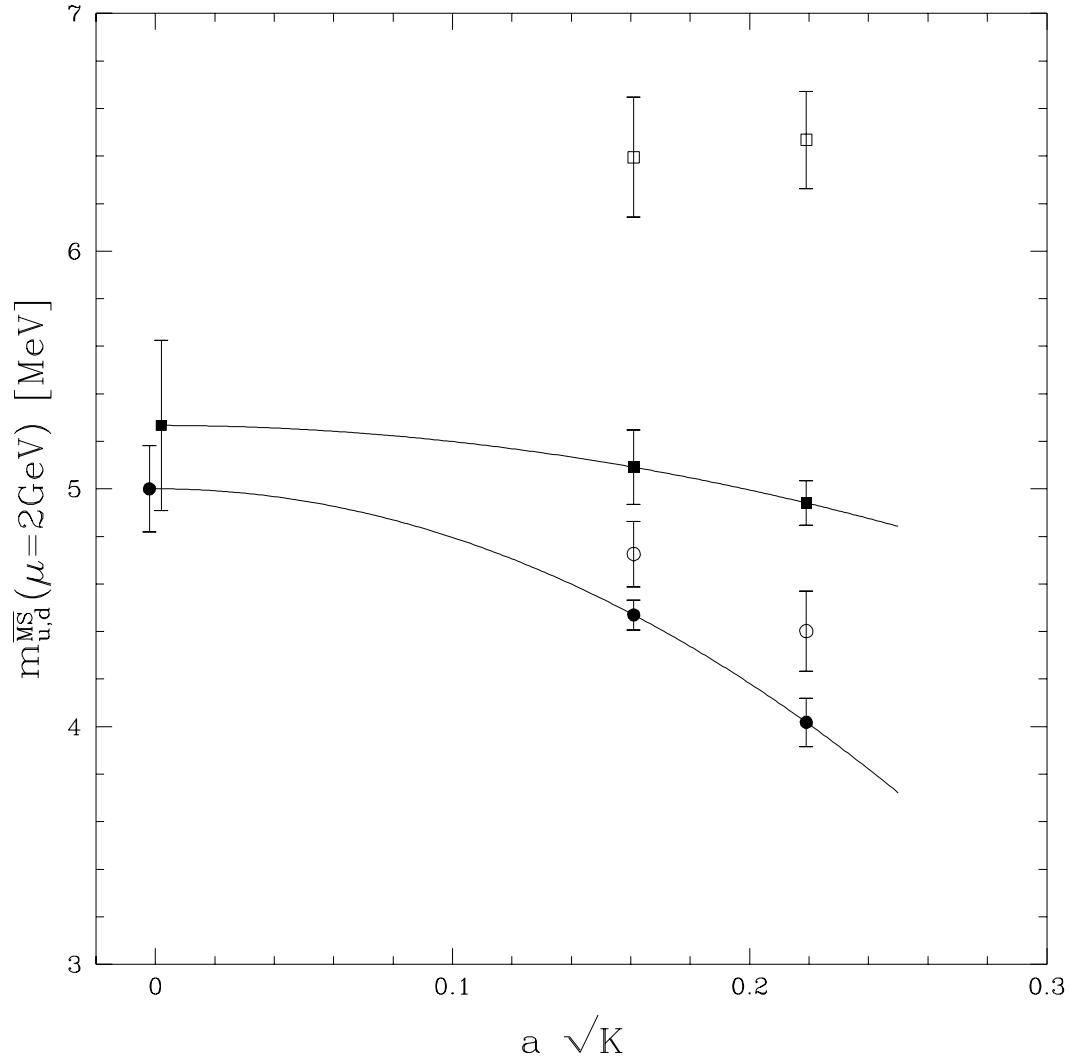


Figure 10: The light quark mass  $m_{u,d}^{\overline{MS}}$  as a function of the lattice spacing for improved fermions using the Ward identity (●) and standard method (■). This is compared with the Wilson result for the Ward identity (○) and standard method (□). The curves are quadratic extrapolations to the continuum limit.



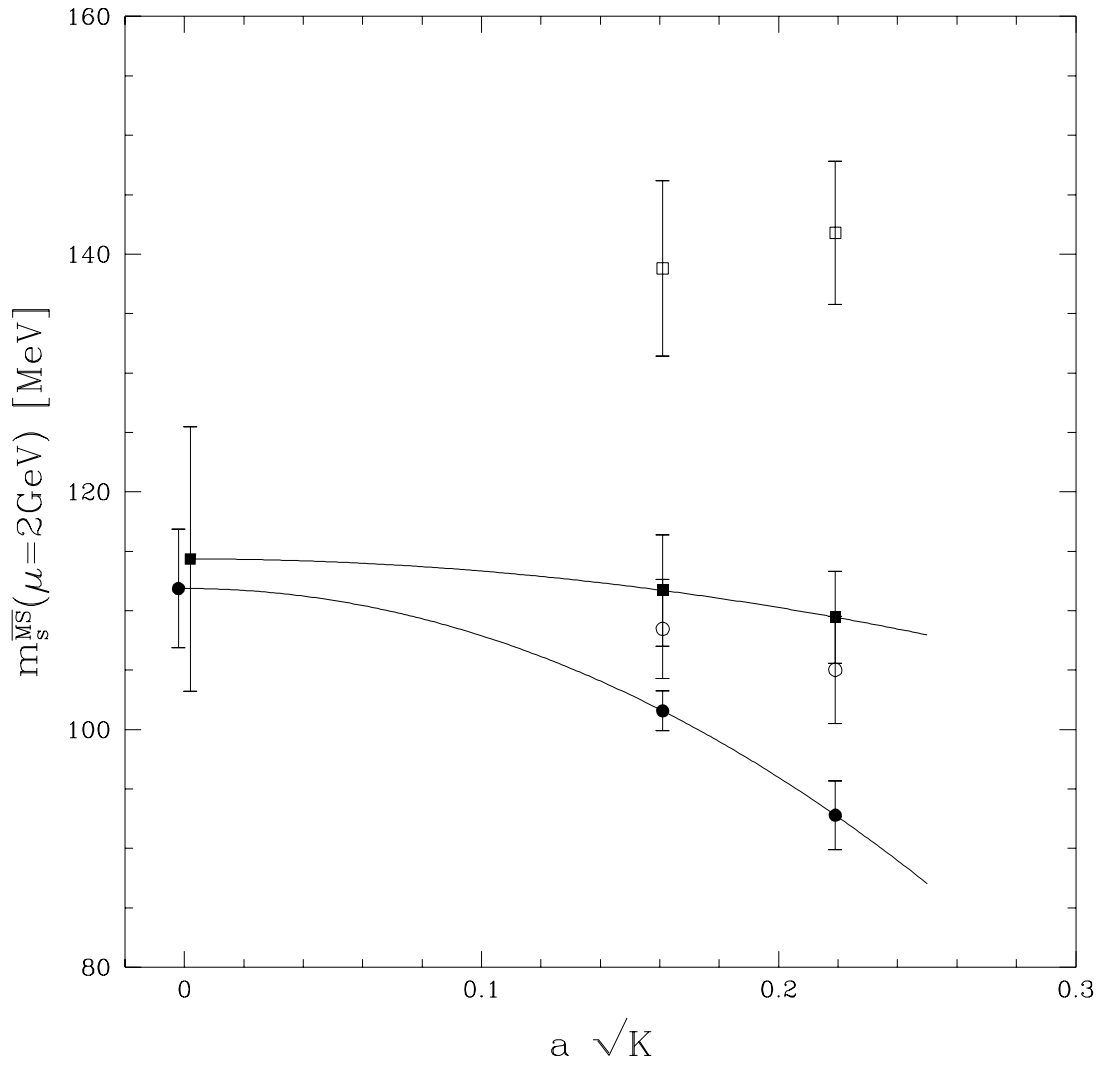


Figure 11: The same as fig. 10 but for the strange quark mass  $m_s^{\overline{MS}}$ .

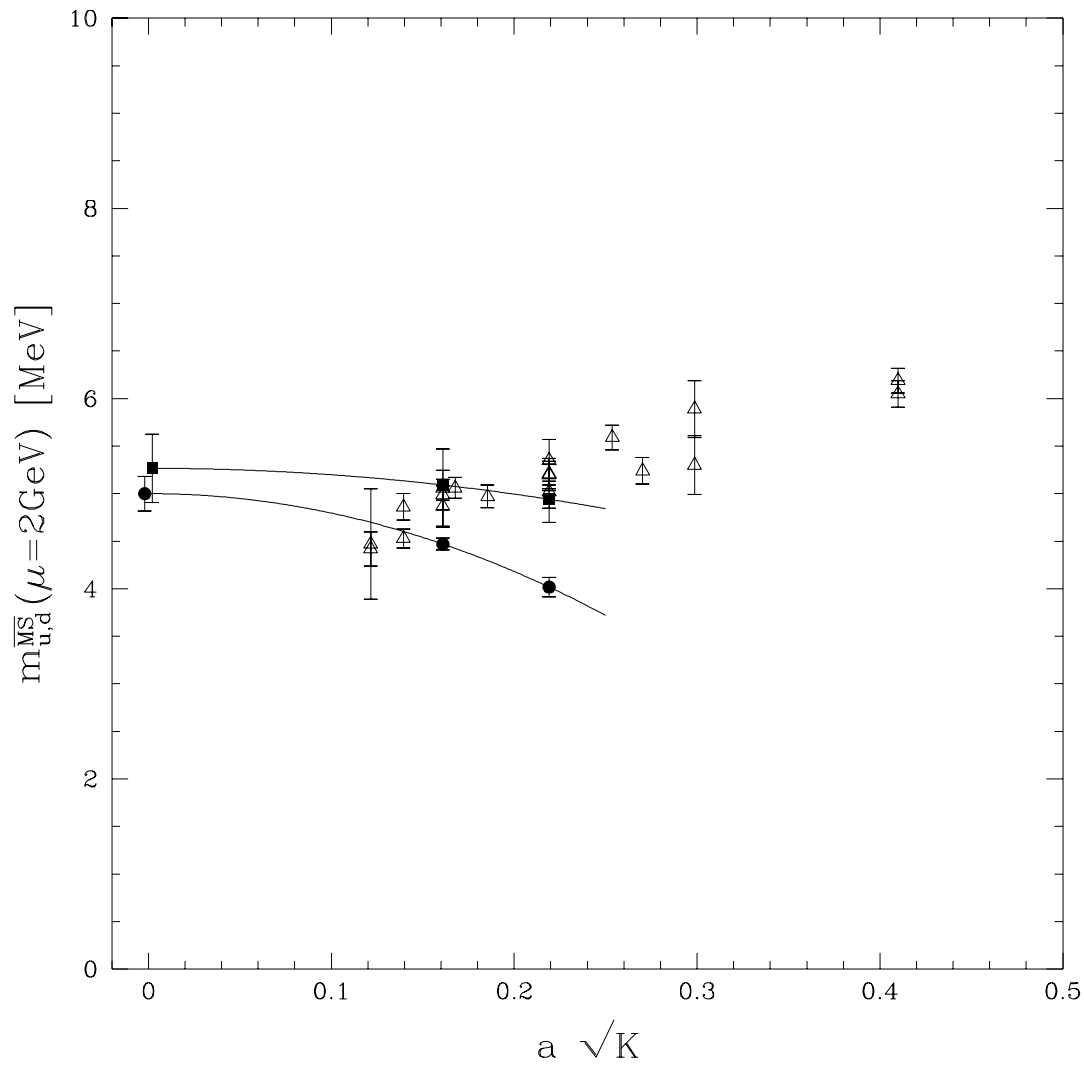


Figure 12: The light quark mass  $m_{u,d}^{\overline{MS}}$  for improved fermions from fig. 10 compared with the world Wilson masses ( $\triangle$ ) compiled in [49].

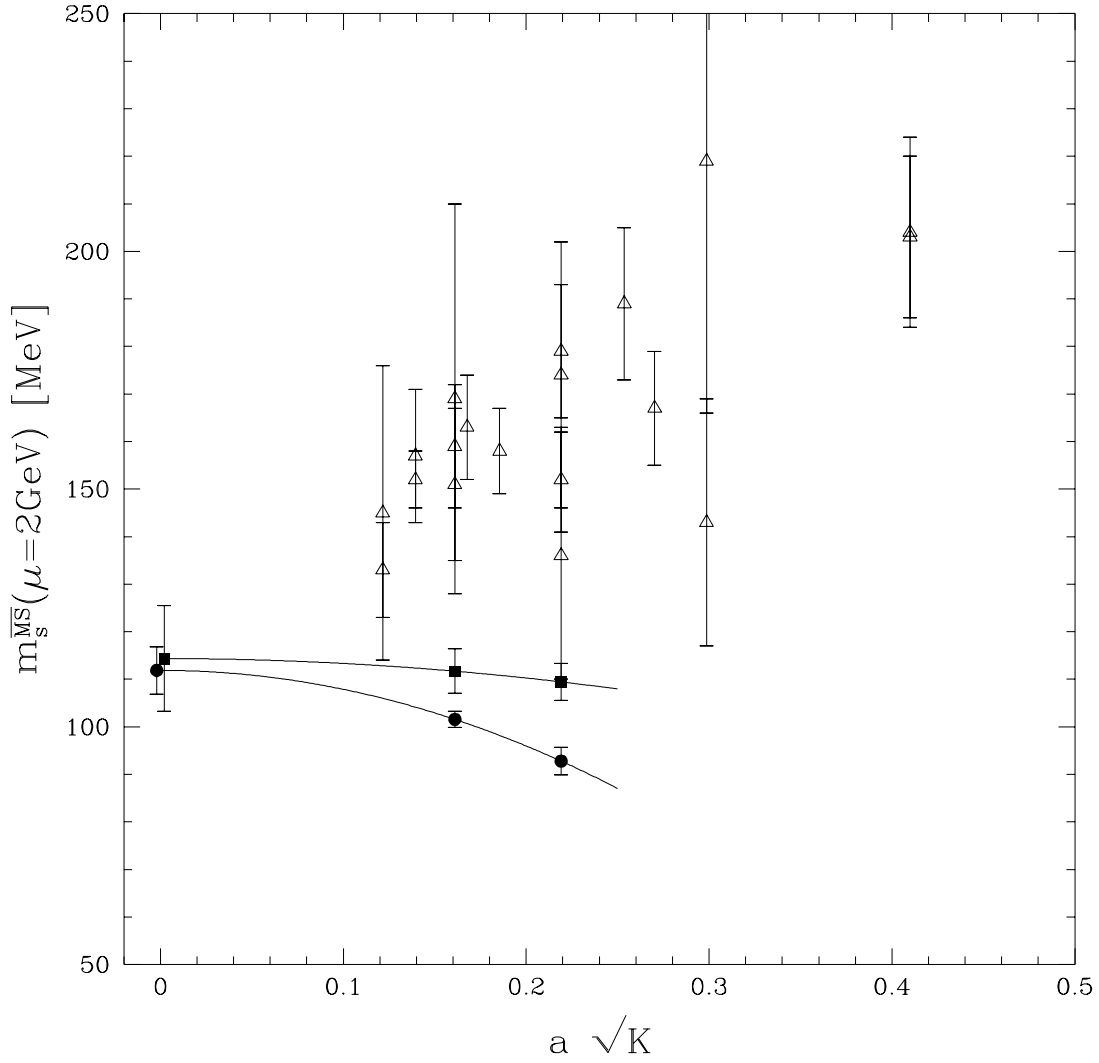


Figure 13: The strange quark mass  $m_s^{\overline{MS}}$  for improved fermions from fig. 11 compared with the world Wilson masses ( $\triangle$ ) compiled in [49]. These authors use the  $\phi(1020)$  meson to determine the strange quark mass.

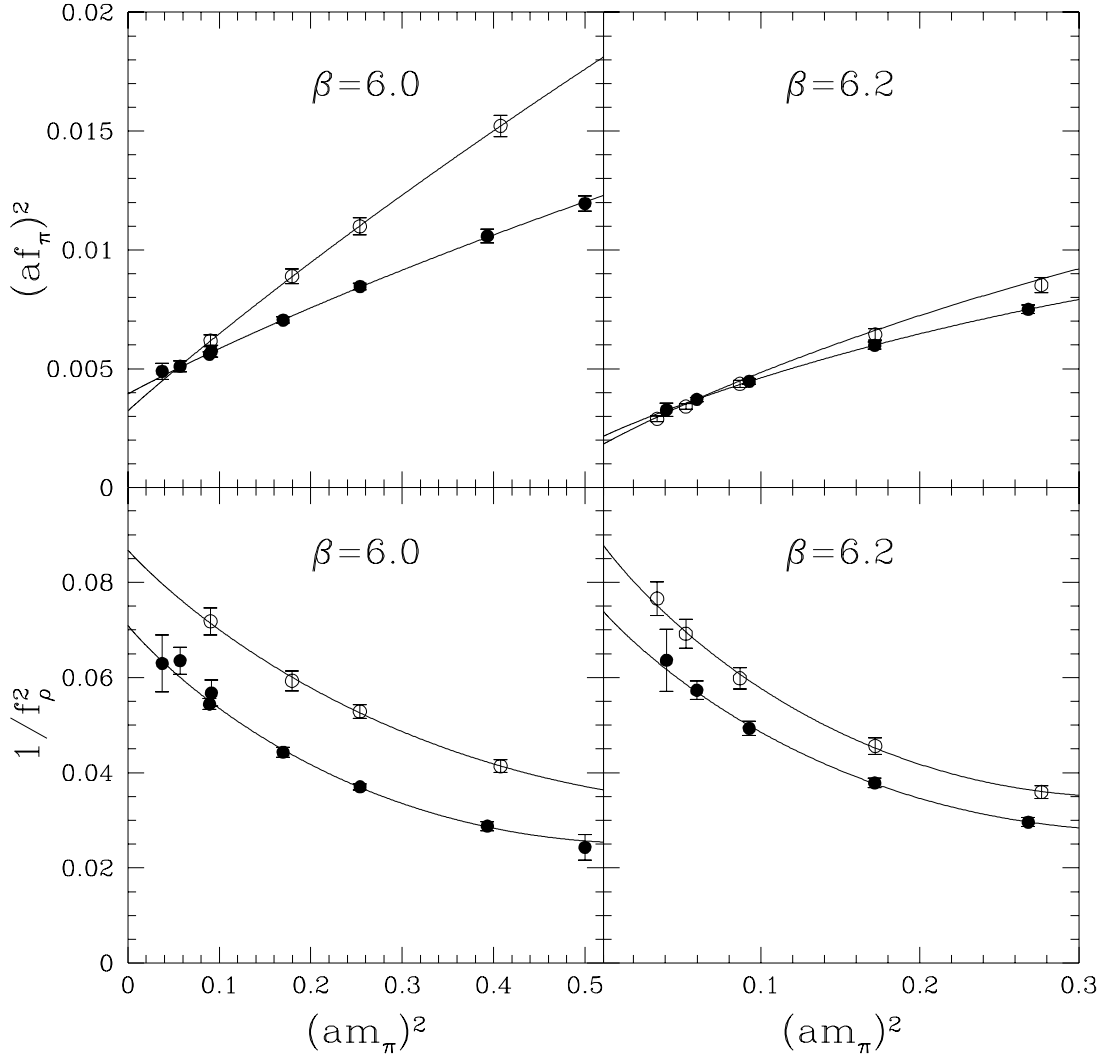


Figure 14: Fits and chiral extrapolations of the decay constants  $f_\pi$  and  $f_\rho$  for improved ( $\bullet$ ) and Wilson ( $\circ$ ) fermions.

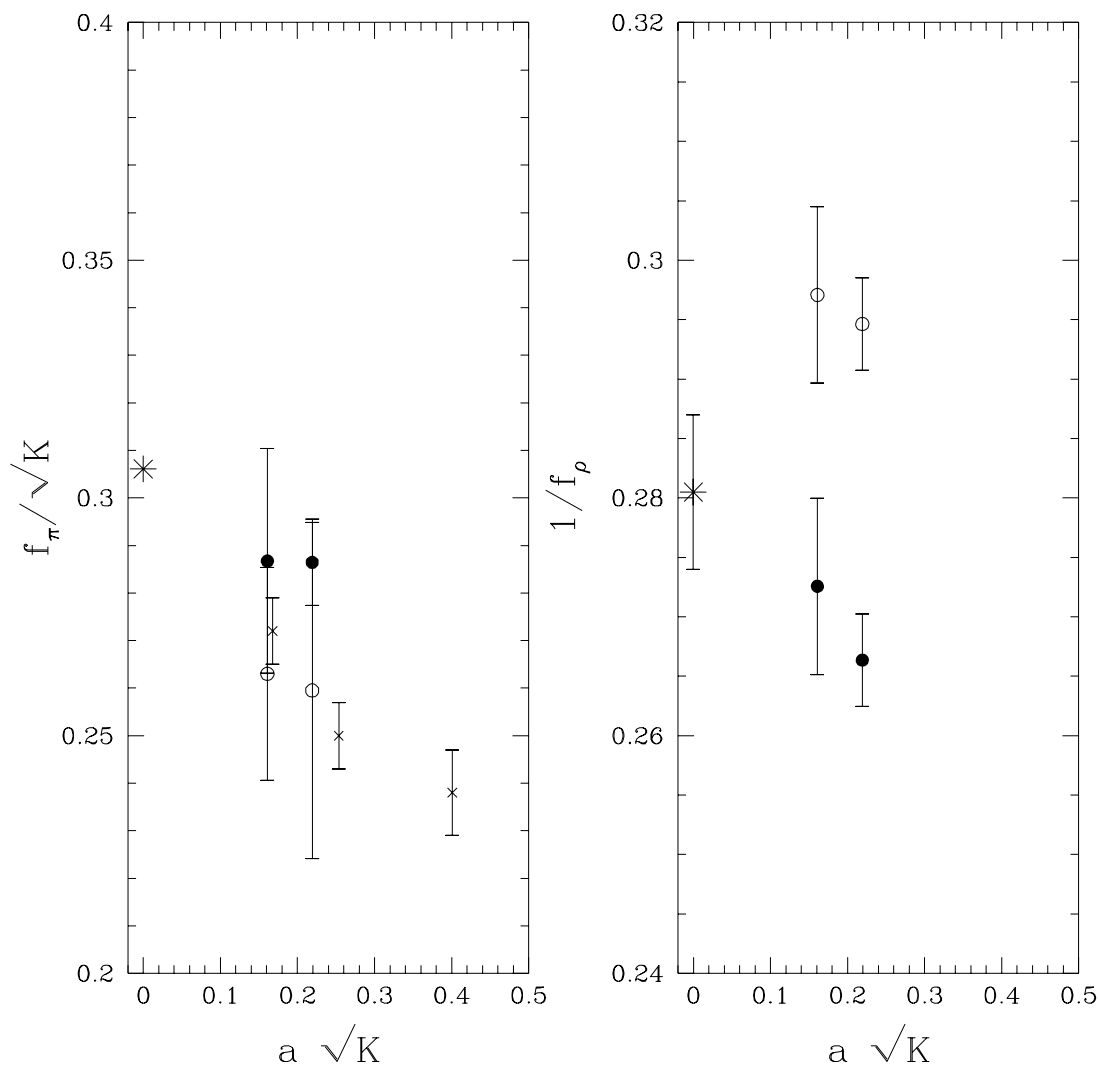


Figure 15: The decay constants  $f_\pi$  and  $f_\rho$  as a function of the lattice spacing for improved (●) and Wilson (○) fermions together with the experimental values (\*). The errors on  $f_\rho$  for improved fermions are statistical only. Our results for  $f_\pi$  are compared with the Wilson results of ref. [51] (×).

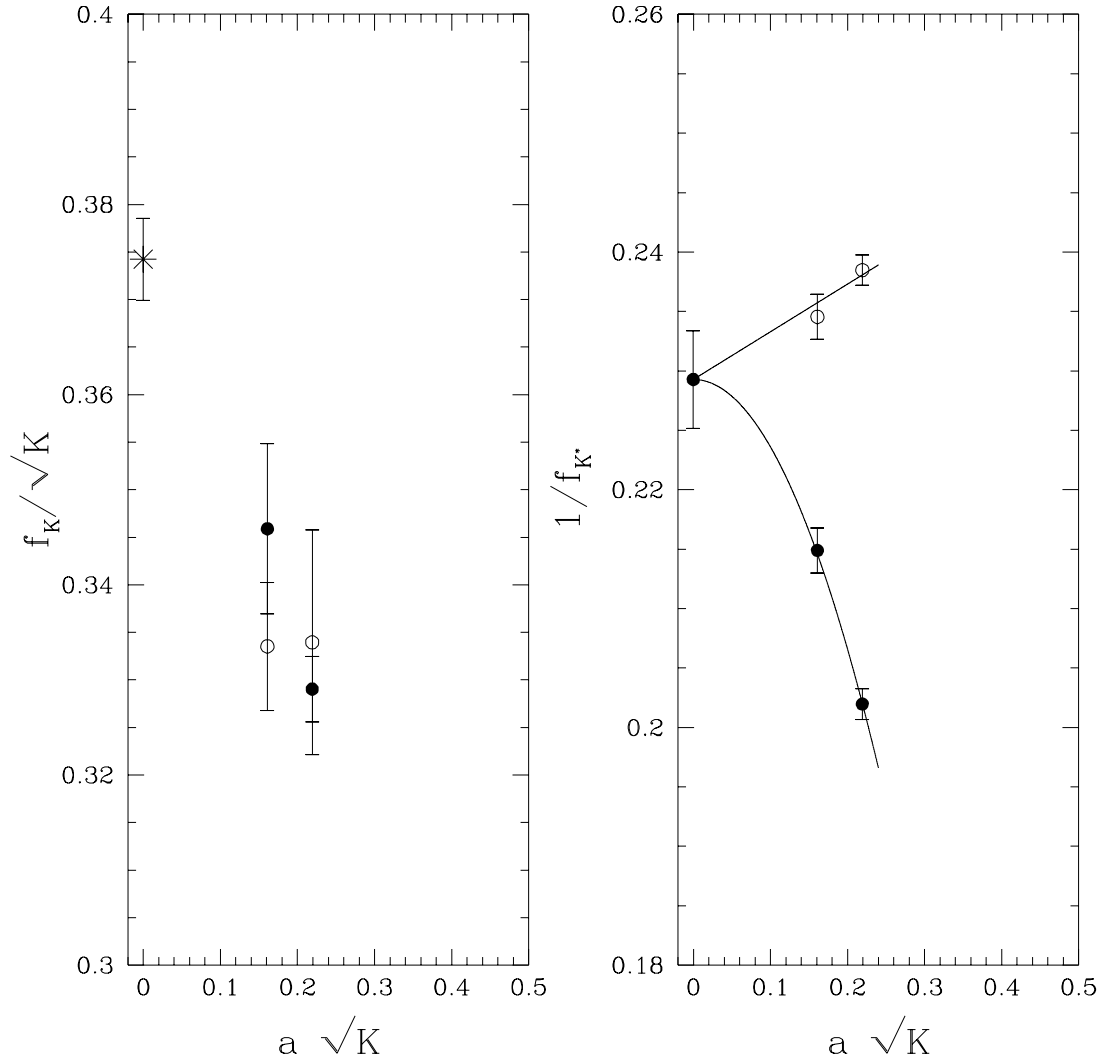


Figure 16: The decay constants  $f_K$  and  $f_{K^*}$  as a function of the lattice spacing for improved (●) and Wilson (○) fermions. The errors on  $f_{K^*}$  for improved fermions are statistical only. The solid lines in the  $f_{K^*}$  figure are from a simultaneous linear fit to the Wilson data and a quadratic fit to the improved data. Our results for  $f_K$  are compared with the experimental value (\*).

## References

- [1] K. Symanzik, Nucl. Phys. B226 (1983) 187, 205.
- [2] M. Lüscher and P. Weisz, Commun. Math. Phys. 97 (1985) 59; erratum: *ibid.* 98 (1985) 433.
- [3] B. Sheikholeslami and R. Wohlert, Nucl. Phys. B259 (1985) 572.
- [4] M. Lüscher, S. Sint, R. Sommer, P. Weisz and U. Wolff, Nucl. Phys. B491 (1997) 323.
- [5] M. Göckeler, R. Horsley, H. Perlt, P. Rakow, G. Schierholz, A. Schiller and P. Stephenson, Phys. Lett. B391 (1997) 388.
- [6] M. Göckeler, R. Horsley, E.-M. Ilgenfritz, H. Perlt, P. Rakow, G. Schierholz and A. Schiller, Nucl. Phys. B (Proc. Suppl.) 42 (1995) 337.
- [7] M. Göckeler, R. Horsley, E.-M. Ilgenfritz, H. Perlt, P. Rakow, G. Schierholz and A. Schiller, Phys. Rev. D53 (1996) 2317.
- [8] M. Göckeler, R. Horsley, E.-M. Ilgenfritz, H. Perlt, H. Oelrich, P. Rakow, G. Schierholz, A. Schiller and P. Stephenson, Nucl. Phys. B (Proc. Suppl.) 53 (1997) 312.
- [9] H. van der Vorst, SIAM J. Sc. Stat. Comp. 12 (1992) 631.
- [10] A. Frommer, V. Hannemann, B. Nockel, T. Lippert and K. Schilling, Int. J. Mod. Phys. C5 (1994) 1073.
- [11] C. Best, M. Göckeler, R. Horsley, E.-M. Ilgenfritz, H. Perlt, P. Rakow, A. Schäfer, G. Schierholz, A. Schiller and S. Schramm, DESY preprint DESY 97-41 (1997) ([hep-lat/9703014](#)), to appear in Phys. Rev. D.
- [12] S. R. Sharpe, Nucl. Phys. B (Proc. Suppl.) 30 (1993) 213.
- [13] D. Weingarten, Nucl. Phys. B (Proc. Suppl.) 34 (1994) 29.
- [14] G. P. Lepage and P. B. Mackenzie, Phys. Rev. D48 (1993) 2250.
- [15] G. S. Bali, Wuppertal preprint WUB 93-37 (1993) ([hep-lat/9311009](#)).
- [16] Ph. de Forcrand, M. Fujisaki, M. Okuda, T. Hashimoto, S. Hioki, O. Miyamura, A. Nakamura, I. O. Stamatescu, Y. Tago and T. Takaishi, Nucl. Phys. B460 (1996) 416.

- [17] P. Bacilieri, E. Remiddi, G. M. Toderico, S. Cabasino, N. Cabibbo, L. A. Fernandez, E. Marinari, P. Paolucci, G. Parisi, G. Salina, A. Tarantcon, F. Coppola, M.-P. Lombardo, E. Simeone, R. Tripiccione, G. Fiorentini, A. Lai, F. Marzano, F. Rapuano and W. Tross, Phys. Lett. B214 (1988) 115;  
M. Guagnelli, M.-P. Lombardo, E. Marinari, G. Parisi and G. Salina, Nucl. Phys. B378 (1992) 616.
- [18] C. R. Allton, V. Gimenez, L. Giusti, and F. Rapuano, Nucl. Phys. B489 (1997) 427.
- [19] S. Collins, Nuc. Phys. B (Proc. Suppl.) 30 (1993) 393.
- [20] F. Butler, H. Chen, J. Sexton, A. Vaccarino and D. Weingarten, Nucl. Phys. B430 (1994) 179.
- [21] Y. Iwasaki, K. Kanawa, T. Yoshie, T. Hoshino, T. Shirakawa, Y. Oyanagi, S. Ichii and T. Kawai, Phys.Rev. D53 (1996) 6443;  
T. Yoshie, Y. Iwasaki, K. Kanaya, S. Sakai, T. Hoshino, T. Shirakawa and Y. Oyanagi, Nucl. Phys. B (Proc. Suppl.) 26 (1992) 281.
- [22] T. Bhattacharya, R. Gupta, G. Kilcup and S. Sharpe, Phys. Rev. D53 (1996) 6486.
- [23] S. Aoki, M. Fukugita, S. Hashimoto, Y. Iwasaki, K. Kanaya, Y. Kuramashi, H. Mino, M. Okawa, A. Ukawa and T. Yoshie, Nucl. Phys. B (Proc. Suppl.) 47 (1996) 354.
- [24] K. M. Bitar, R. G. Edwards, U. M. Heller, A. D. Kennedy, T. A. DeGrand, S. Gottlieb, A. Krasnitz, J. B. Kogut, W. Liu, P. Rossi, M. C. Ogilvie, R. L. Renken, D. K. Sinclair, R. L. Sugar, D. Toussaint and K. C. Wang, Phys. Rev. D46 (1992) 2169.
- [25] M. Fukugita, Y. Kuramashi, M. Okawa and A. Ukawa, Phys. Rev. Lett. 75 (1995) 2092.
- [26] J. N. Labrenz and S. R. Sharpe, Nucl. Phys. B (Proc. Suppl.) 34 (1994) 335.
- [27] R. Sommer, Nucl. Phys. B411 (1994) 839.
- [28] R. Sommer, Phys. Rep. 275 (1996) 1.
- [29] G. S. Bali and K. Schilling, Phys. Rev. D47 (1993) 661.
- [30] S. P. Booth, D. S. Henty, A. Hulsebos, A. C. Irving, C. Michael and P. W. Stephenson, Phys. Lett. B294 (1992) 385.
- [31] H. Wittig, Nucl. Phys. B (Proc. Suppl.) 42 (1995) 288.
- [32] H. Hoerber (1997): ref. [29] reanalyzed with link integration.



- [33] C. R. Allton, C. T. Sachrajda, R. M. Baxter, S. P. Booth, K. C. Bowler, S. Collins, D. S. Henty, R. D. Kenway, C. McNeile, B. J. Pendleton, D. G. Richards, J. N. Simone, A. D. Simpson, A. McKerrell, C. Michael and M. Prisznyak, Nucl. Phys. B407 (1993) 331.
- [34] S. Perantonis and C. Michael, Nucl. Phys. B347 (1990) 854.
- [35] K. D. Born, R. Altmeyer, W. Ibes, E. Laermann, R. Sommer, T. F. Walsh and P. M. Zerwas, Nucl. Phys. B (Proc. Suppl.) 20 (1991) 394.
- [36] E. Eichten, K. Gottfried, T. Kinoshita, K. D. Lane and T. M. Yan, Phys. Rev. D21 (1980) 203.
- [37] M. Camprostrini and C. Rebbi, Phys. Lett. B193 (1987) 78.
- [38] For a review see for example: M. Neubert, CERN preprint CERN-TH/96-292 (1996) (hep-ph/9610266).
- [39] H. Pagels, Phys. Rev. D19 (1979) 3080.
- [40] Review of Particle Physics, Particle Data Group, Phys. Rev. D54 (1996) 1.
- [41] M. Lüscher, S. Sint, R. Sommer and P. Weisz, Nucl. Phys. B478 (1996) 365.
- [42] M. Lüscher, S. Sint, R. Sommer and H. Wittig, Nucl. Phys. B491 (1997) 344.
- [43] S. Sint and P. Weisz, MPI preprint MPI-PhT/97-21 (1997) (hep-lat/9704001).
- [44] S. Capitani, M. Göckeler, R. Horsley, H. Perlt, P. Rakow, G. Schierholz and A. Schiller, in preparation.
- [45] M. Göckeler, R. Horsley, H. Oelrich, H. Perlt, P. Rakow, G. Schierholz and A. Schiller, in preparation.
- [46] H. Leutwyler, Phys. Lett. B378 (1996) 313.
- [47] M. Göckeler, R. Horsley, H. Oelrich, H. Perlt, P. Rakow, G. Schierholz and A. Schiller, Nucl. Phys. B (Proc. Suppl.) 47 (1996) 493.
- [48] S. Aoki, M. Fukugita, S. Hashimoto, N. Ishizuka, Y. Iwasaki, K. Kanaya, Y. Kuramashi, H. Mino, M. Okawa, A. Ukawa and T. Yoshiè, Nucl. Phys. B (Proc. Suppl.) 53 (1997) 209.
- [49] R. Gupta and T. Bhattacharya, Phys. Rev. D55 (1997) 7203.
- [50] R. Sommer, CERN preprint CERN-TH/97-107 (1997) (hep-lat/9705026).

- [51] F. Butler, H. Chen, J. Sexton, A. Vaccarino and D. Weingarten, Nucl. Phys. B421 (1994) 217.
- [52] M. Wingate, T. DeGrand, S. Collins and U. M. Heller, Phys. Rev. Lett. 74 (1995) 4596.